의학 박사 학위논문

ADHD brain network during development

: animal ^{18}F-FDG PET and human fMRI study

발달 과정에서의 ADHD 뇌 네트워크의 연구

: 소동물 ^{18}F-FDG PET 및 소아-청소년 fMRI 연구

2018년 2월

서울대학교 융합과학기술대학원

분자의학 및 바이오제약학과

하 승 균

Abstract

ADHD brain network during development

: animal ^{18}F-FDG PET and human fMRI study

Seunggyun Ha

Department of Molecular Medicine and Biopharmaceutical Science,

The Graduate School of Convergence Science and Technology,

Seoul National University

Attention-deficit hyperactivity disorder (ADHD) is a complex brain developmental disorder characterized by hyperactivity/impulsivity and/or inattention. These ADHD patients are known to be defective in terms of compensation and motivation, and it is known that there is a problem in the connectivity between the prefrontal and striatum. . In addition, the suppression of the default mode network (DMN) in the ADHD brain network is not normally performed. In addition, recent advances in ADHD network analysis revealed that differences in ADHD brain network like less inhibition of default mode network (DMN) cause the brain dysfunction in ADHD. There are several hypotheses about the cause of ADHD, and the explanation that the normal maturation is delayed is supported by various studies, but the evidence for this is mainly the anatomical study on the development of cortical thickness. The main aim of this study is to evaluate the hypothesis of "delayed maturation" using metabolic and functional connectivity analysis.

In this study, a longitudinal study of metabolic connectivity using rat 18F-FDG PET imaging and a functional connectivity cross-sectional analysis using human fMRI data were performed. SHR rats were selected as the ADHD model, WKY rats were used as controls, and ^{18}F-FDG PET brain images were taken at 4 weeks of age (childhood) and at 6 weeks of age (entry of puberty). ADHD-200 public human fMRI data especially from Peking University was collected to compare typically developing control (TDC) and ADHD patients according to age criteria of 12 years-old.

The SHR rats exhibited a variety of phenotypes. Twelve SHR rats showing distinct impulsivity and activity were selected as ADHD rats through behavior tests of marble burying test, open field test, and delay discouting task. The brain images of 12 ADHD rats and 12 control rats were analyzed. When voxel-based analysis was performed, ADHD rats and control rats were not significantly different from each other even during development from 4 weeks to 6 weeks (FWE >0.05). When the changes in the metabolic connectivity during development were evaluated using the persistent homology analysis, rat network analysis showed enhancement of the limbic (hippocampus) and cerebral cortical connections ($P < 0.05$, permutation 10000). In ADHD rats, enhancement of the limbic (medial olfactory cortex) -cortical cortex, which was significantly weakened compared with the same 4-week-old control group, was observed during this development ($P < 0.05$, permutation 10000). In addition, the connection between hippocampus and cerebral cortex also tended to be enhanced during ADHD development ($P < 0.10$, permutation 10000). When the 4-week-old control group and the 6-week-old ADHD rat brain metabolic connectivity were compared, there was no significant difference in the network except for the weakening of the inter-thalamic linkage. Characteristically, during the development from 4 weeks to 6 weeks of age, ADHD rats were delayed in modulating the reward-motivation area (striatum, medial prefrontal cortex, and anterior cingulate cortex)

compared to the control group.

The connectivity analysis of fMRI data using persistent homology showed that the functional connectivity between children and adolescents in the TDC was significantly strengthened throughout the brain (FDR <0.05). On the other hand, the ADHD group showed localized differences of connections, and there was no significant change in the overall functional network formation pattern evaluated by the area under the curve of the barcode using persistent homology (FDR >0.05). On the other hand, there was no gross difference between the TDC group and ADHD group (FDR >0.05).

Finally, we analyzed the information flow efficiency of the rat metabolic networks and the human functional networks by using volume entropy as an index. The volume entropy of the ADHD rats was lower than that of the control rats with same age. The development of ADHD rats from 4 weeks to 6 weeks of age was relatively limited but developed. When the human functional networks were analyzed, the volume entropy was significantly increased with age in the TDC group (r 0.240, P = 0.006). In contrast, the ADHD group showed no significant difference in age-related volume entropy (P >0.05). There was no statistically significant difference of volume entropy between the TDC and ADHD groups (P >0.05).

In conclusion, the analysis of the metabolic network in the developmental process of the ADHD rat model revealed that delayed enhancement of the connectivity between the limbic-cerebral cortex, which partially supported the 'delayed mature hypothesis'. And the volume entropy, the overall information flow efficiency was also delayed during maturation of the ADHD rats. In the functional network study in the ADHD-200 cohort, the ADHD group showed little difference in age compared to the TDC group. A longitudinal study with appropriate medication control is needed to validate the delayed maturation hypothesis in ADHD’ in human data.

Keywords: ADHD, delayed maturation, brain connectivity, persistent homology, volume entropy, ^{18}F-FDG PET, fMRI

Student Number: 2014-30805

Contents

Abstract……1

Contents……...5

List of tables……...8

List of figures……9

List of abbreviations……...11

Introduction……....13

ADHD……13

Brain network analysis……14

Purpose……17

Materials and methods……..18

Metabolic network analysis in ADHD rats……18

Animal models……..18

Behavioral tests and ADHD phenotype-(+) rat selection……..18

^{18}F-FDG PET imaging……19

Preprocessing of rat brain ^{18}F-FDG PET……22

Voxel-wise regional analysis……....22

Anatomical parcellation of rat brain……22

Brain metabolic network construction……23

Graph filtration using persistent homology……..23

Permutation for SLM comparison……28

Functional network analysis in ADHD patients……28

ADHD-200 project……...……28

Network construction and comparison of single linkage distance……29

Efficiency of information processing on a network……30

Volume entropy calculation……..……30

Application of volume entropy……..……30

Statistics……...…33

Results ……34

Part I. Brain metabolic network analysis in ADHD rat model……..34

ADHD-phenotype expression in rat models……34

Voxel-wise comparison of metabolic activity in ADHD rat brain……38

Persistent homology analysis in metabolic network in rat models……..…40

Difference of metabolic network in rat models……43

Modularization of brain network during development……48

Part II. Brain functional network analysis in ADHD……51

Demographics of ADHD-200 cohort……51

Construction of functional individual SLM ……54

Difference of interregional connections during development……..57

Part III. Maturation of metabolic network based on volume entropy……59

Change of volume entropy during maturations in rat models……..……59

Comparison of volume entropy in human fMRI data……61

Discussion……64

Conclusion……..…67

Acknowledgment……68

Conflict of interest……..…69

References……..……70

국문초록……..……....79

List of tables

Table 1. Results of voxel-wise comparison …….39

Table 2. Demographics of subjects from ADHD-200 cohort…….....52

Table 3. Comparison of demographics of ADHD subjects (8-12y vs. 12-15y).....53

Supplemental table 1. Analyzed ROIs on the rat template (Schiffer)…… 76

Supplemental table 2. Analyzed ROIs on the human AAL template…….77

List of figures

Figure 1. Scheme of animal experiment that PET imaging and behavioral tests…..21

Figure 2. Persistent homology with a hypothetical example of weighted graph with 6 nodes…….25

Figure 3. Scheme of brain network analysis using persistent homology……..27

Figure 4. Volume entropy calculated on universal covering tree……..32

Figure 5. Marble-burying test at 5-wk age between SHR and WKY…….....35

Figure 6. Selection of ADHD-phenotype (+) rats…….....36

Figure 7. Correlation, distance, and single-linkage matrices of the ADHD rat group and the normal control group at 4wk and 6wk ages……..…….41

Figure 8. Graph filtration of the ADHD rat group and the normal control group at 4wk and 6wk ages…….42

Figure 9. SLM difference with 10000-permuted test ($P < 0.05$).....44

Figure 10. Difference of SLM between the SHR-6wk and the WKY-6wk with 10000 permutation test ($P < 0.10$)……45

Figure 11. Comparison of SLM between SHR-6wk and WKY-4wk……46

Figure 12. Single linkage dendrograms of rat brain metabolic networks……47

Figure 13. Minimum spanning tree of the control rats and ADHD rats……49

Figure 14. Circular plots of MSTs in the control rats and ADHD rats.....50

Figure 15. Barcodes of subjects in $TDC_{8\text{-}12y}$, $TDC_{12\text{-}15y}$, $ADHD_{8\text{-}12y}$, and $ADHD_{12\text{-}15y}$…….....55

Figure 16. Comparison of area-under curves of barcodes for TDC and ADHD….56

Figure 17. Comparison of SLDs among $TDC_{8\text{-}12y}$, $TDC_{12\text{-}15y}$, $ADHD_{8\text{-}12y}$, and $ADHD_{12\text{-}15y}$……..58

Figure 18. Volume entropy with varying thresholds on rat metabolic network.....60

Figure 19. Correlation plot between age and individual volume entropy……62

Figure 20. Comparison of functional individual volume entropy in TDC and ADHD during development……..63

List of abbreviations

Full name	*Abbreviations*
ACC	Anterior cingulate cortex
ADHD	Attention-deficit hyperactivity disorder
β0	Betti-0, number of connected components
CP	Caudoputamen
DAN	Dorsal attention network
DDT	Delay discounting task
DMN	Default mode network
FDR	False discovery rate
^{18}F-FDG	^{18}F-Fluorodeoxyglucose
fMRI	Functional magnetic resonance imaging
FWE	Family-wise error
Lt	Left
MBT	Marble burying test
mPFC	Medial prefrontal cortex
OFT	Open field test
PCC	Posterior cingulate cortex
PET	Positron-emission tomography
r	Pearson correlation coefficient or radius
ROI	Region of interest
rsfMRI	Resting state functional magnetic resonance imaging
Rt	Right
SHR	Spontaneously hypertensive rat (ADHD model)
SHR_in	SHR rats included in the network analysis
SHR_out	SHR rats excluded from the network analysis

SLD	Single linkage distance
SLM	Single linkage matrix
sqrt	Square root
TDC	Typically developing control
wk	Week or week-age
WKY	Wistar Kyoto rat (Control)

Introduction

ADHD

Attention-deficit hyperactivity disorder (ADHD) is one of the most common brain developing disorder which is clinically marked by key inappropriate behaviors like inattention and/or hyperactivity/impulsivity (1). The ADHD prevalence is approximately 5-10% of school-aged children (2, 3). Once ADHD was believed that it is limited to childhood/adolescence, but 65% of school-aged ADHD cases persists to adulthood (4, 5). ADHD gives negative impact to affect subjects and families because it is related to poor achievement in academic domains and persistence in adult is a significant factor of poor socioeconomic outcome and comorbid psychiatric disorders (5-8). Psychostimulants, particularly, methylphenidate are the treatment of choice in ADHD management, which provides short-term improvement of symptoms and academic achievement (9). The pathophysiological understanding to ADHD is limited, but the polygenetic nature of ADHD has been acknowledged (10). In addition to genetic factors, several environmental factors including food, cigarette and alcohol exposure, and maternal smoking during pregnancy have been proposed as risk factors (11).

So far, the pathophysiological mechanism of ADHD has not been fully unveiled, although recent neuroimaging studies provide advanced information about ADHD. Based on the anatomical analysis, the individuals with ADHD had subcortical brain volume differences that smaller sized bilateral amygdala, nucleus accumbens, and hippocampus (12). Even though multiple potential loci of the brain are thought to be related to a heterogenous developmental condition of ADHD, recent evidence suggests that dysfunction of interregional connectivity affects ADHD (13). The hypoactivation of the fronto-striatal circuit in ADHD, which mediates executive functions, has been widely evaluated and supported by multiple studies (14-16).

Recently, it has been suggested that diminished inhibition of the default mode network (DMN) which comprises medial prefrontal cortex (mPFC), posterior cingulate cortex (PCC), precuneus, and lateral posterior parietal brain regions are associated with ADHD (17-20). In general, the DMN network increased activity during resting state and decreased activity during cognitive task (21). The inhibition of DMN is mainly mediated by the dorsal attention network (DAN) which modulate goal-directed voluntary (top-down) executive processes (22), and many studies have shown that abnormality in the DAN is related to ADHD (16, 23). In patients with ADHD, psychostimulants normalized the reduced fronto-striatal activity and improved inhibition of DMN during cognitive tasks (24, 25).

Based on the observation of connectivity patterns in ADHD, it resembles the connectivity of younger typically developing subjects (26, 27), so a hypothesis has been suggested that ADHD is a delay of maturation rather than an abnormality. Although the delayed maturation hypothesis has become one of the main hypothesis explaining ADHD with structural evidence of cortical thickening delay (28-30), there is less knowledge about the change in the maturation process of the brain metabolic and/or functional network in ADHD. Considering having difficulty in repeatedly imaging of ADHD cases from the same subject, the preclinical experiment is expected to give new knowledge. The spontaneously hypertensive rat (SHR) is a well-studied animal model of ADHD with symptoms of hyperactivity, impulsivity and learning deficits (31).

Brain network analysis

The brain is a complex functional organ composed of a bunch of neural bundles. Brain networks could be topologically analyzed based on graph theory, which is called brain graph (32). Defining nodes and edges are the elemental part of

constructing brain graph. The results of brain graph analysis, brain connectivity, is dependent on the scale of measurement from the level of individual neurons (microscale) to cortical regions, lobes, and systems (macroscale) (33). The brain is a multiscale organ, and each scale analysis provides important information about brain connectome. At the microscale, graph theory interprets microscopic findings of neurons and synapses as nodes and edges, respectively. This attempts revealed that brain network organization seems to evolve to minimize axonal wring cost (34). The microscopic analysis presents advantages of high spatial and temporal resolution but also disadvantages of invasiveness. Also, the measurement of microscopic findings is not scalable for the larger scaled neural system. At the macroscopic scale, non-invasive imaging techniques such as electroencephalography (EEG), magnetoencephalography (MEG), fMRI, and positron emission tomography (PET) are applied to measure neurophysiological signals to estimate large-scale functional networks. With the rapid development of imaging and analysis techniques, neuroimaging studies have revealed more knowledge to understand brain network at the macroscopic scale (35). At macroscale analysis, regions-of-interest (ROIs), nodes, are determined heuristically based on cytoarchitecture and anatomical landmarks (36, 37). Large-scale functional connectivity is estimated by measuring the statistical dependence of neurophysiological signals between two nodes on imaging methods. To obtain the statistical dependence between nodes, the Pearson correlation coefficient which represents linear correlation has been widely used. A high correlation of neurophysiological signals like hemodynamic signals on fMRI or ^{18}F-fluorodeoxyglucose (^{18}F-FDG) uptake on PET between two nodes indicates in-phase coupling.

When performing brain network analysis, signals of each brain area obtained from imaging modality were analyzed and construct a network by forming a connection when the correlation exceeds a certain threshold (38). However, this method has a

high degree of arbitrariness in determining a specific threshold because there is no gold standard. Additionally, an interregional connection with a low degree of correlation also contains information of brain network (39). A graph filtration method over changing thresholds which is called persistent homology provides threshold-free brain network analysis without loss of information from applying certain thresholds and has been used for variable modalities including MEG, T1-MR, and ^{18}F-FDG PET in multiple disorders (40-43). Meanwhile, volume entropy is a newly suggested parameter defined as the exponential growth rate of paths on the assumption that the information flows infinitely through a network. Based on the definition, volume entropy level is an indicator of the efficiency of information processing on a brain network.

Purpose

The purpose of this study was to evaluate the change of brain metabolic network in a rat model to validate the delayed-maturation theory in ADHD. Open-source fMRI data, ADHD-200, was analyzed to validate the results from the animal PET study. Also, the maturation of brain network in ADHD and typically developing cases in preclinical and clinical data were described by a newly suggested parameter, volume entropy.

Materials and methods

Metabolic network analysis in ADHD rats

Animal models

The Institutional Animal Care and Use Committee at Seoul National University approved all animal care and experiments for this research. SHR, a representative animal model of ADHD and Wistar Kyoto rat (WKY), control were used for brain network analysis using ^{18}F- FDG PET in rats (44). Thirty-four SHRs and 12 WKY rats were used for animal experiments including brain ^{18}F-FDG PET imaging and behavioral tests. The animals were kept at standard laboratory condition (22-24℃, 12 hour light and dark cycle) with no restriction of standard feeding and water-drinking.

Behavioral tests and ADHD phenotype-(+) rat selection

The overall scheme of animal imaging and behavioral tests was displayed in Figure 1. Three behavioral tests were performed to check phenotype-expression of ADHD. A marble burying test (MBT) to assess the degree of disruptive behavior and impulsivity was done at the rat-age of 5 weeks around the age for PET imaging. The rats were allowed to acclimate the test rat cages individually with pine wood bedding at least 15 minutes before the MBT tests. Fifteen glass marbles were evenly spaced as 3 x 5 array on the pine wood bedding in each test cage. The rats were tested individually in the test cage with placed marbles for 15 minutes. After removal of the rats from the cages, the number of buried marbles more than 50% or more covered by bedding was counted. At the rat-age of 8 to 9 weeks, an open field test (OFT) to assess hyperactivity was tested for each rat. Individual rats were placed in

the 40 cm x 40 cm sized black box for the OFT. The behavior of each rat was tracked via a video camera installed above the open-filed apparatus during 30 minutes. The moved distance of each rat was recorded every 10 minutes. The total moved distance was adopted as the result of OFT. The delay discounting task (DDT) for the impulsive choice of a rat was tested also at the rat-age 8 to 9 weeks. Before the DDT test, each rat was stabilized as 5 days of habituation in the animal room with free available food. After stabilization, food was restricted for 2 days. Each rat trained two levers which returned a different amount of food delivery. One lever returned a food pellet immediately as a small and immediate reward. The other lever returned five food pellets as a large reward. After delivery of food, 20 seconds of illumination was given as timeout periods. No food pellet was returned for the lever presses during the time-out periods. During adjusting delay sessions, food was restricted as 5g of pellet per 100g of body weight for every one hour except after tests. Each test was performed for 30 minutes in a day. A delay was inserted for the lever with the large rewards and sequentially increased over the test days (0, 10, 20, 30, and 40 seconds). A percentage of choice for the large reinforce was recorded for each day. The mean percentage of choice for the larger reinforce with delays of 20 to 40 seconds was adopted as a result of the DDT. The results of three behavioral tests were reviewed synthetically, and twelve SHR rats which are matched to the number of WKY rats were selected as ADHD-phenotype-(+) rats. To select ADHD-phenotype-(+) rats, exclusion criteria that lower rank (0-25%) per each trial of any three behavioral tests was applied.

^{18}F-FDG PET imaging

^{18}F-FDG PET imaging of rat brain was performed at dual age-points, 4 week-age and 6 week-age considering childhood and adolescent age (45). Dedicated small

animal PET/computed tomography (CT) scanner (eXplore VISTA, GE Healthcare, WI) was used for PET imaging. Overnight fasting was done before PET imaging. Before 45 minutes of PET imaging, ^{18}F-FDG (150-220 MBq/kg) were injected intravenously after anesthetization by 2% isoflurane at 1.5-2 L/min oxygen flow for 5 minutes. Each Rat was awake and took rest in a dark room for 35 minutes. Static PET imaging was started 45 minutes after ^{18}F-FDG injection. Stating PET scan was acquired for 20 minutes with the energy window 250-700 keV. A three-dimensional ordered-subsets expectation maximum (OSEM) algorithm with attenuation, random, and scatter correction was used for image reconstruction. The voxel size was 0.3875× 0.3875× 0.775 mm^3.

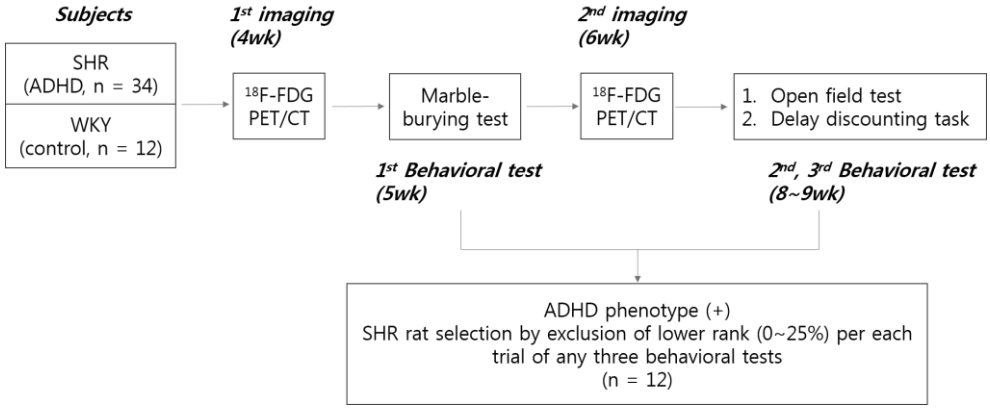

Figure 1. Scheme of animal experiment that PET imaging and behavioral tests

The overall scheme of the animal experiment was composed of two times of PET imaging at 4wk- and 6wk-age and three times of behavioral tests that marble-burying test, open field test, and delay discounting task.

Preprocessing of rat brain ^{18}F-FDG PET

For preprocessing, all voxels were scaled by a factor of 10 in each dimension. Brain PET images were manually realigned to the rat brain MRI T1 template using PMOD 2.7 (PMOD group, Zurich, Switzerland) (46). After realignment, smoothing with a Gaussian filter of 6 mm full width at half maximum (FWHM) was applied to all brain PET images to adjust image qualities. Spatial alignment using non-linear registration on Statistical Parametric Mapping (SPM8, University College of London, London, UK) was performed using single channel using the rat brain PET template (46) and binary brain mask. Smoothing with a Gaussian filter of 12 mm FWHM was applied to the spatially normalized images. The voxel counts were normalized to the global brain uptake in each PET image.

Voxel-wise regional analysis

A paired t-test was applied to analyze the change of regional metabolic activity during maturation from 4-week to 6-week of rat-age in the rat groups of WKYs or SHRs. Also, two sample t-test was applied to compare the difference of regional activity between the different rat groups with same age. The family-wise error (FWE) of 0.05 which is a corrected p-value for multiple comparison corrections was used to determine significance. In the regional analysis, minimum 50 voxels were regarded as a statistically significantly different region.

Anatomical parcellation of rat brain

The ROIs for rat brain were defined by Schiffer template which was presented by PMOD 2.7 (PMOD group, Zurich, Switzerland). Among the 58 ROIs defined by the

Schiffer template, 32 ROIs including cortices (frontal, parietal, occipital, temporal, and insula) and limbic structures were selected for analysis. The cerebellar ROIs were excluded from the analysis. Detailed information of ROIs including full name, abbreviations, and displayed orders in this study were explained in the supplemental table 1.

Brain metabolic network construction

To construct a weighted undirected brain metabolic network, each ROI was regarded as a node. In each group, a positive correlation matrix (Cx, 32 x 32) among 32 nodes of rat brain on ^{18}F-FDG PET scans was obtained using the Pearson correlation coefficient (r_{ij}, r_{ij} >0) between certain two nodes (p_i, p_j). Distance matrix (Dx, 32 x 32) in each group was defined by the following formula.

$$\mathrm{Dx} = \mathrm{sqrt}(1 - \mathrm{Cx})$$

Graph filtration using persistent homology

Edge, a connection between two nodes is defined when the correlation between nodes exceeds a predetermined correlation threshold. In other words, two nodes are connected when a distance between two nodes was less than a predetermined distance threshold. The persistent homology method using graph filtration over changing threshold of distance was applied to avoid biased results by arbitrary determination of threshold (40). Figure 1 explains the concept of persistent homology by using an example of a weighted graph with 6 nodes. Persistent homology obtains the number of connected components, Betti-0 (β0), which quantifies a topological property of network. With the distance threshold of 0, the

number of β0 is same to the number of ROIs. While changing thresholds for connection of nodes from strict to loose, β0 has values from the number of ROIs to 1. The changes in β0 are visualized by barcodes and dendrograms. While changing thresholds, a graph of monotonically decreasing β0 from the number of ROIs to one is referred as a barcode in this article (Figure 2A). The dendrogram shows the hierarchical connection between ROIs along the changing thresholds. The filtration value which allows a connection between two brain regions (separately connected components) is defined as single linkage distance (SLD) of newly connected nodes. The SLDs between all nodes can be displayed in the single linkage distance matrix (SLM) (Figure 2B). As well as barcodes, single linkage dendrograms, and SLMs, the minimum spanning tree (MST) which is a unified subgraph calculated to allow the overall shortest edges by considering most important edges between nodes during graph filtration was obtained. Figure 3 explains the flow of brain network analysis using the persistent homology.

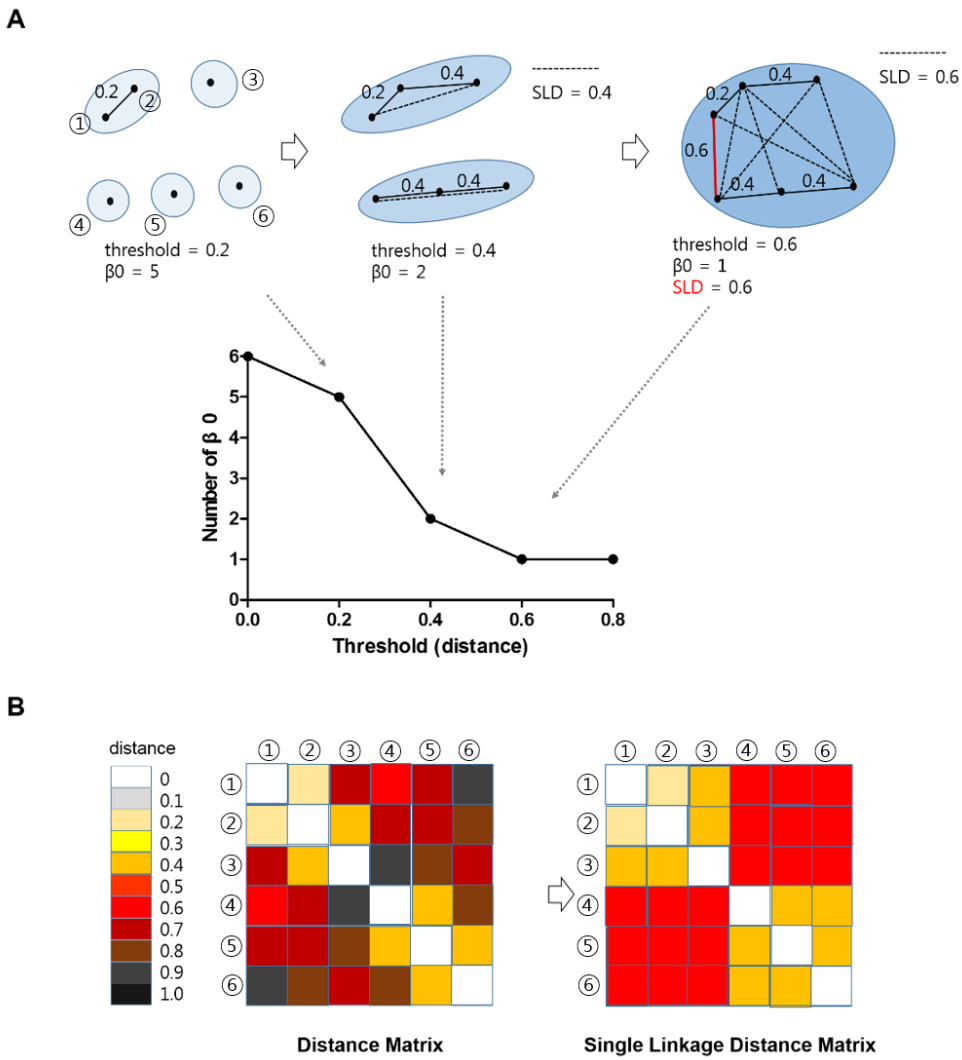

Figure 2. Persistent homology with a hypothetical example of weighted graph with 6 nodes

With varying filtration of distance thresholds, serial connections with different distance are constructed among 6 nodes. When a new connection (red line) is constructed with the loosening of the threshold from a distance 0.4 to 0.6, SLD between nodes which are not directly linked but within the connected component

(dotted lines) is determined as same to the SLD of the new linkage. The number of connected components, β0 can be visualized as a barcode (A). Distance matrix for the 6 nodes can be converted to SLM according to the definition of SLD (B). Abbreviations: SLD, single linkage distance; SLM, single linkage distance matrix

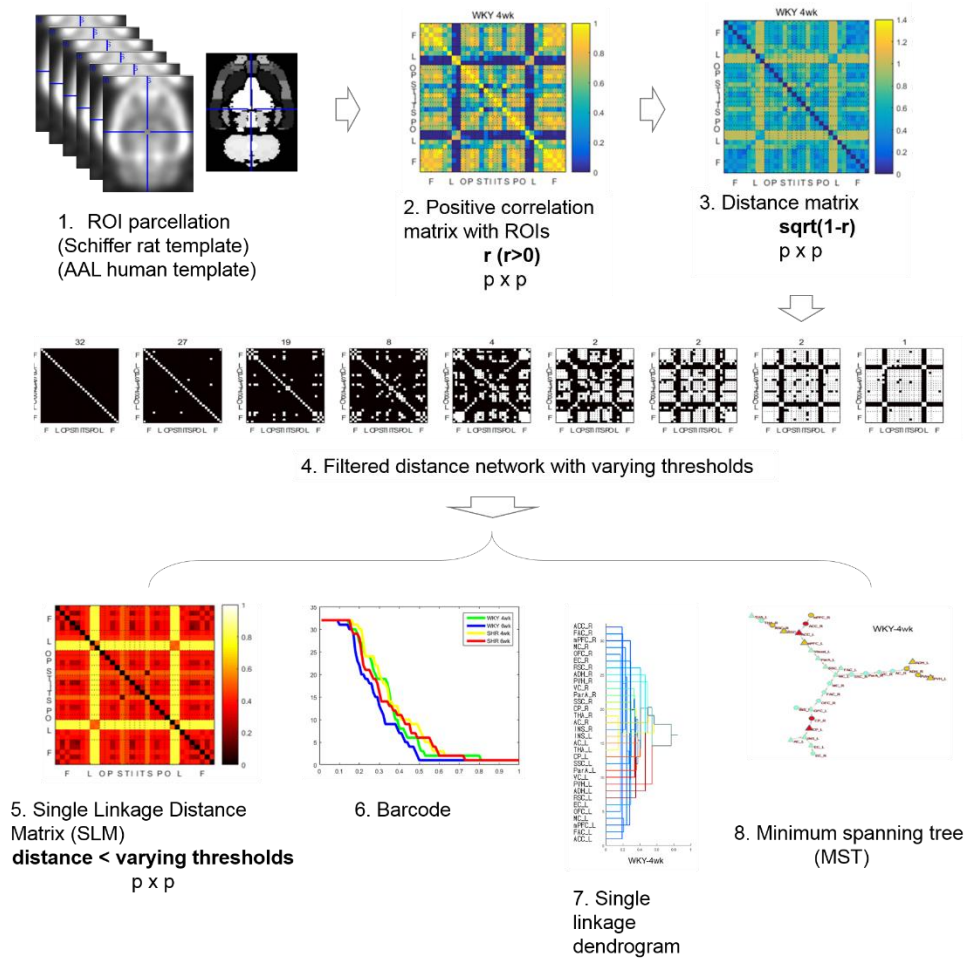

Figure 3. Scheme of brain network analysis using persistent homology

Brain network analysis with filtration free approach of persistent homology was displayed as a flowchart. The brain images were parcellated by a predetermined ROIS on anatomical brain template. The correlation degree between ROIs calculated as Pearson correlation coefficients (r) were displayed on a correlation matrix. After conversion of correlation matrix to a positive correlation matrix, a distance matrix was determined as the predetermined definition that sqrt(1-r). With subgraphs obtained by all available varying thresholds, SLM, barcode, single linkage dendrogram, and MST were obtained.

Permutation for SLM comparison

SLMs and barcodes of β0 were constructed with randomly reassigned labels (i.e., ADHD or control) and permuted 10,000 times as a permutation test of our comparisons of correlation maps in the above. Type I errors were calculated by the comparison of the observed differences in SLDs in the ADHD/control groups for each connection and the distributions in SLD differences from the permuted data. We used $P < 0.05$ to find interregional connections in VOI pairs showing significantly different SLDs (dij) between the ADHD and control groups.

Functional network analysis in ADHD patients

ADHD-200 project

The publicly released database, ADHD-200 Sample (http://fcon_1000.projects.nitrc.org/indi/adhd200/) was used for this analysis. The NeuroBureau (http://neurobureau.projects.nitrc.org/ADHD200/) released the preprocessed fMRI data which was conducted according to the following routine steps using the packages AFNI (afni.nimh.nih.gov/afni) and FSL(www.fmirb.ox.ac.uk/fsl/) running on the Athena computer cluster at Virginia Tech's ARC: 1) remove first 4 EPI volumes 2) slice time correction 3) deoblique dataset, 4) reorient into RPI orientation, 5) Motion correct EPI volumes to the first image of the time series 6) mask the dataset to exclude non-brain, 7) Average the volumes to create a mean image, 8) co-register mean EPI image to corresponding anatomic image 9) write fMRI data and mean image into template space at 4 mm x 4 mm x 4 mm resolution, 10) down-sample WM and CSF masks (from anatomical preprocessing) to match EPI resolution, 11) extract WM and CSF time-courses from EPI volumes using WM and CSF masks, 12) regress out WM, CSF, motion time

courses (calculated from motion correction) as well as a low order polynomial (detrending) from EPI data, 13) band-pass filter ($0.009 < f < 0.08$ Hz) voxel timecourses to exclude frequencies not implicated in resting state functional connectivity, 14) Blur the filtered and unfiltered data using a 6-mm FWHM Gaussian filter. The ROIs were defined using the AAL parcellation. Among the preprocessed fMRI data from seven different institutions, the data from Peking university which contains total 245 cases of fMRI of typically developing control (TDC) and ADHD was chosen. Among them, 132 cases of TDC and 91 cases of ADHD were analyzed because the rest excluded was not satisfying quality control or was an extraordinary case about volume entropy by Tukey's method using x1.5 interquartile range. The subjects from ADHD-200 cohort was subdivided by the age of 12 years for classification of childhood and adolescent. Therefore, 4 groups that $TDC_{8\text{-}12y}$ (age 8-12y), $TDC_{12\text{-}15}$ (age, 12-15y), $ADHD_{8\text{-}12y}$ (age 8-12y), and $ADHD_{12\text{-}15y}$ (age, 12-15y) were included in this analysis.

Network construction and comparison of single linkage distance

Construction of matrices of positive correlation, distance, and SLD of 90 AAL ROIs excluding cerebellum was serially conducted for each subject of the included ADHD-200 fMRI data, in the same manner, explained in the animal data analysis. Barcodes by persistent homology were drawn for all subjects. Evaluation of group comparison of SLD for each ROI was conducted in two ways as a same mental diagnosis with different age ($TDC_{8\text{-}12y}$ vs. $TDC_{12\text{-}15y}$ or $ADHD_{8\text{-}12y}$ vs. $ADHD_{12\text{-}15y}$) and different mental status with same age ($TDC_{8\text{-}12y}$ vs. $ADHD_{8\text{-}12y}$ or $TDC_{12\text{-}15y}$ vs. $ADHD_{12\text{-}15y}$).

Efficiency of information processing on a network

Volume entropy calculation

Volume entropy suggests topological quantity representing the efficiency of transferring information on a network. Volume entropy is based on a universal covering tree which is an infinite connected network without any terminal node (Figure 4). Universal covering tree preserves degree at every node and weight of every edge on original network. All possible paths with radius r on universal covering tree without backtracking starting with a base node v_0 is denoted as $B(v_0, r)$. Volume entropy h_{vol} is sum the of all edge-weights when r comes to infinite number and is defined as following formula:

$$h_{vol} = \lim_{r\to\infty} \frac{\log l(B(v_0,r))}{r} \quad (47)$$

To calculate volume entropy, a brain graph should satisfy the following condition that degree of all nodes should be equal or larger than 3. Also, the value of volume entropy is highly dependent on the number of edges and eventually dependent on the number of nodes. So, here, the number of edges and nodes were fixed by using spanning-tree subgraph with a 1-nearest neighbor to calculate volume entropy. At the condition, the number of edges, q, are always determined by the number of nodes, p, as following formula:

$$q = p * (p-1)$$

Application of volume entropy

For ADHD rat models, volume entropy was calculated for weighted distance matrix with varying threshold in each group of WKY-4wk, WKY-6wk, SHR-4wk, and SHR-6wk. Also, volume entropy was calculated for weighted distance matrix for

individual subjects of ADHD-200 cohort.

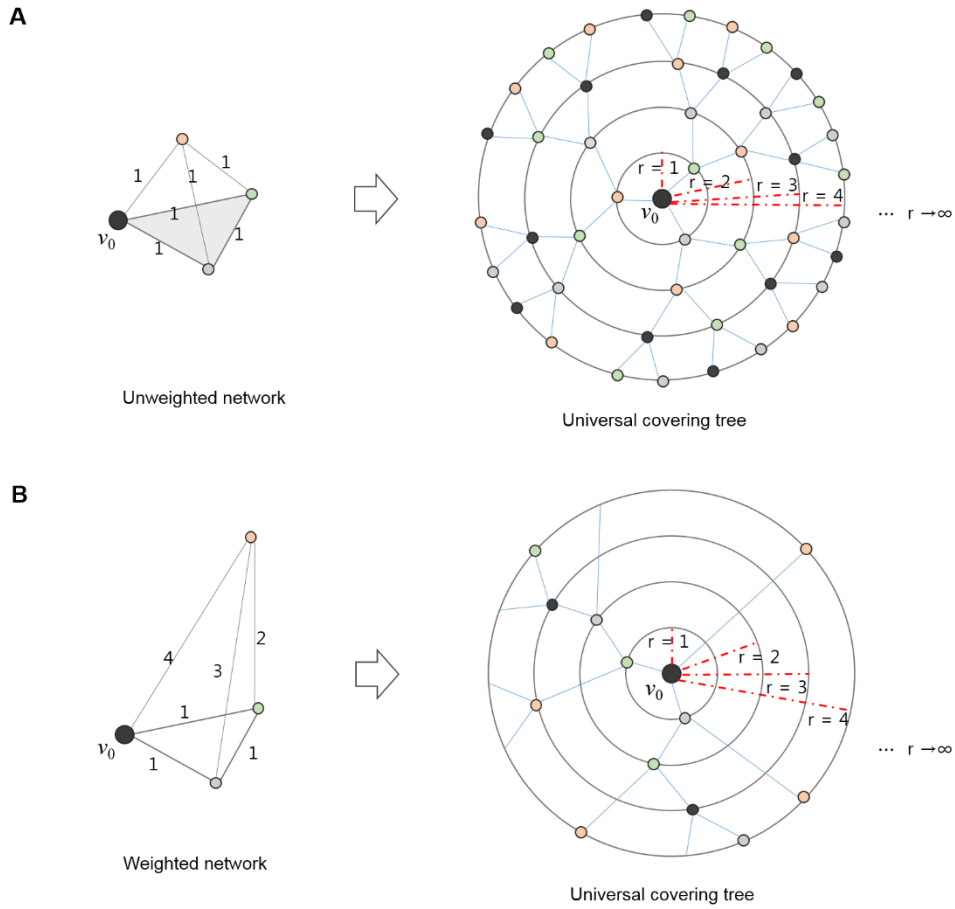

Figure 4. Volume entropy calculated on universal covering tree

Closed networks composed of 4 nodes and 6 edges are converted to infinite networks preserving original nature of each node (degree) and edge (unweighted [A] or weighted strength [B]), which are called universal covering tree. Universal covering tree can be explained as all possible footprints of a random walker who starts on a base node of v_0 on the network. Volume entropy is calculated as a representation of the sum of all edge weights on universal covering tree. Note: r, radius; v_0, starting base node.

Statistics

A permutation test (x10000) was applied to compare interregional connections on SLM between the SHR group and/or WKY group. Area-under-curve (AUC) of barcodes were obtained to compare networks by persistent homology in TDC and ADHD with each age criterion. To compare the group difference of SLD in each ROI of ADHD-200 fMRI data, a non-parametric test that rank-sum test was applied. To adjust multiple comparison issues, FWE rate less than 0.05 was determined as a significant finding in the group comparison of SLD in each ROI using ADHD-200 fMRI data. Correlation between age and volume entropy was analyzed using Pearson correlation coefficient, r. To compare the group differences of volume entropy in ADHD rat data or ADHD-200 fMRI data, ANOVA test was applied with post-hoc analysis of Tukey method. A P-value less than 0.05 was adopted as a significant level of the analysis.

Results

Part I. Brain metabolic network analysis in ADHD rat model

ADHD-phenotype expression in rat models

Impulsivity and disruptive behavior, the typical characteristics of ADHD, were confirmed by a marvel burying test at 5 week-aged. Results of the marble burying test showed significant impulsivity and disruptive behavior in the SHR group compared to the WKY group (P = 0.012) (Figure 5). Therefore, the ADHD phenotype of SHRs appeared at the age of PET imaging. Twelve SHR rats (SHR_in) with more impulsivity and hyperactivity based on the results of MBT, OFT, and DDT were chosen as the ADHD-phenotype (+) group. The SHR_in rats (12.5 ± 2.6) buried significantly more marbles compared to the WKY rats (2.8 ± 2.1, P <0.001) and the excluded SHRs (SHR_out, 5.8 ± 4.8, P <0.001) (Figure 6A). The SHR_in rats (5.0 m ± 1.5 m) showed significantly more movement during the OFT compared to the SHR_out rats (3.6 m ± 1.3 m, P = 0.010). There was a trend of more movement of the SHR_in rats than the WKYs (3.8 m ± 1.6 m) (P = 0.079) (Figure 6B). In the DDT test, the SHR_in rats chose a large reward less frequently compared to the WKY rats significantly (mean percentage of the choices of a large reward, 12.8% ± 8.2% vs. 35.8% ± 33.3%, P = 0.030). The SHR_out rats showed tendency of relatively frequent choice of large reward (mean, 30.5% ± 28.0%) compared to the SHR_in (P = 0.082) (Figure 6C).

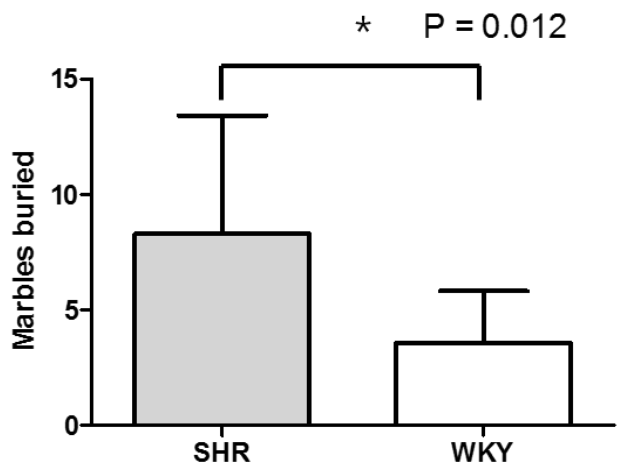

Figure 5. Marble-burying test at 5-wk age between SHR and WKY

The ADHD-model (SHR) buried significantly more marbles than the control group (WKY) in a marble burying test at 5-wk rat age (P = 0.012).

Abbreviations; SHR, spontaneously hypertensive rat; WKY, Wistar Kyoto rat

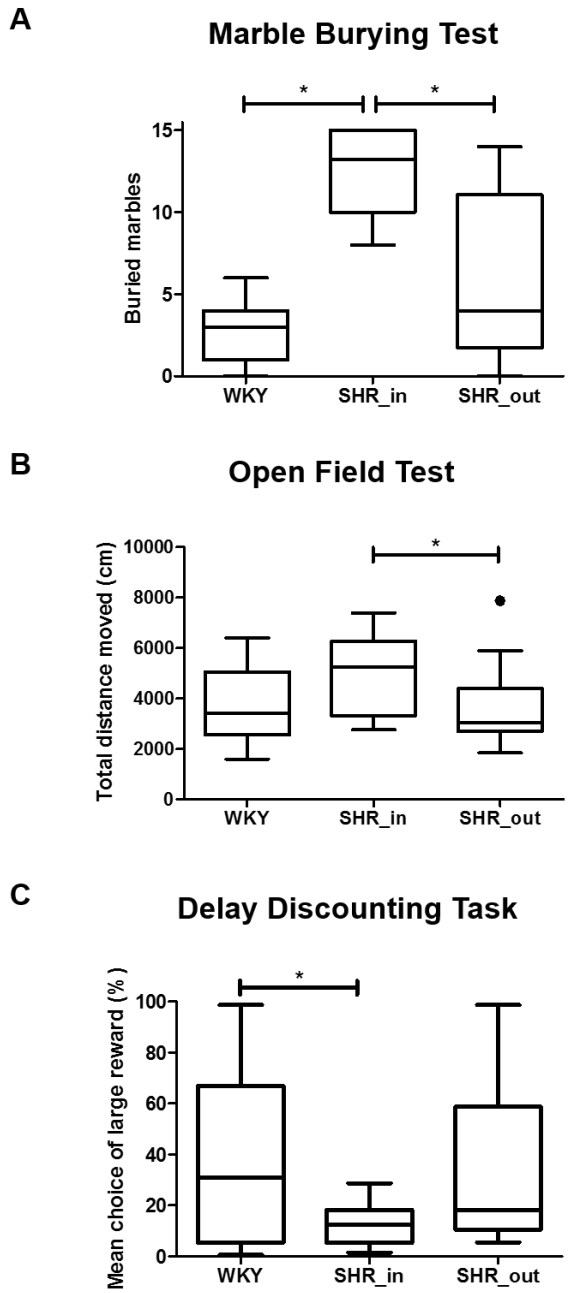

Figure 6. Selection of ADHD-phenotype (+) rats

The impulsivity and hyperactivity of rats were tested by the behavioral tests of MBT (A), OFT (B), and DDT (C). According to the results, 12 cases of SHR rats (SHR_in)

which had more impulsivity and hyperactivity were selected for brain metabolic network analysis. Abbreviations: DDT, delay discounting task; MBT, marble burying test; OFT, open field test; SHR, spontaneously hypertensive rat; SHR_in, SHR rats included in the network analysis; SHR_out, SHR rats excluded from the network analysis; WKY, Wistar Kyoto rat

Voxel-wise comparison of metabolic activity in ADHD rat brain

By the visual analysis of ^{18}F-FDG PET brain images, there was no difference among each group of WKY-4wk, WKY-6wk, SHR-4wk, and SHR-6wk. The voxel-wise comparison using the paired t-test also showed no difference between the groups of WKY-4wk and WKY-6wk (FWE >0.05). Also, the SHR-6wk group had increased regional metabolic activity in the right hippocampus area compared to the SHR-4wk group (FWE >0.05). There was no statistical difference in regional metabolic activity between the WKY-4wk and SHR-4wk groups, or the WKY-6wk and SHR 6-wk groups (FWE >0.05) (Table 1).

Table 1. Results of voxel-wise comparison

Group comparison	FWE <0.05
WKY-4wk vs. WKY-6wk	No difference
SHR-4wk vs. SHR-6wk	No difference
WKY-4wk vs. SHR-4wk	No difference
WKY-6wk vs. SHR-6wk	No difference

Abbreviations: FWE, family-wise error; SHR, spontaneously hypertensive rat; WKY, Wistar Kyoto rat

Persistent homology analysis in metabolic network in rat models

The correlation matrices (Figure 7A) and distance matrices (Figure 7B) were obtained from the brain ^{18}F-FDG PET images in the 4 groups that WKY-4wk, WKY-6wk, SHR-4wk, and SHR-6wk. With filtration methods using all available thresholds on the distance matrices, the SLMs were constructed (Figure 8C). When the threshold of distance was changed from 0.01 to 0.99 in each group, a monotonical change of the number of β0 in each group was shown as a barcode graph (Figure 8A). According to the barcode graphs, there were trends that normal and matured rats had the fast construction of overall brain connections. The serial changes in metabolic networks from early connections to distance connections in each group were displayed in Figure 8B.

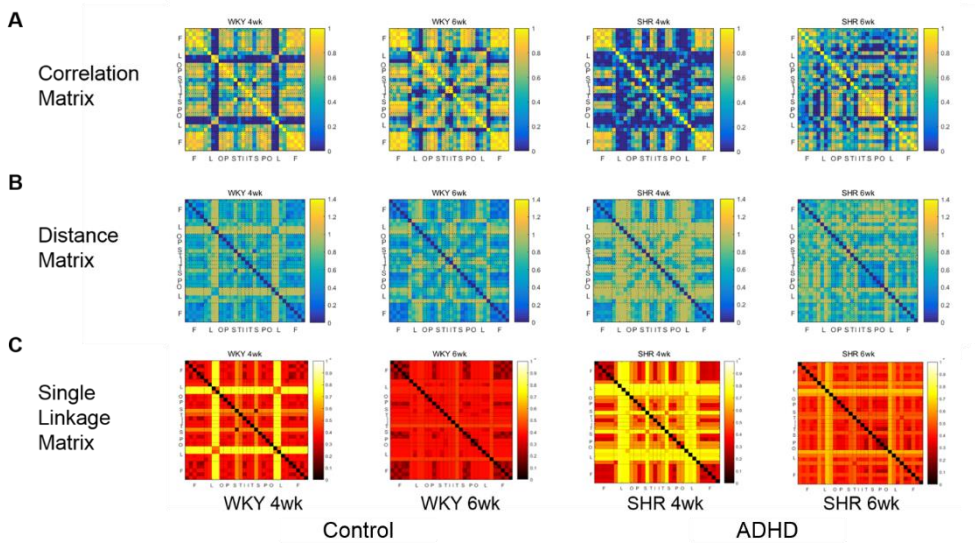

Figure 7. Correlation, distance, and single-linkage matrices of the ADHD rat group and the normal control group at 4wk and 6wk ages

The positive correlation (A), distance (B), and single-linkage (C) matrices using the 32 ROIs were serially constructed in the 4 groups that WKY-4wk, WKY-6wk, SHR-4wk, and SHR-6wk.

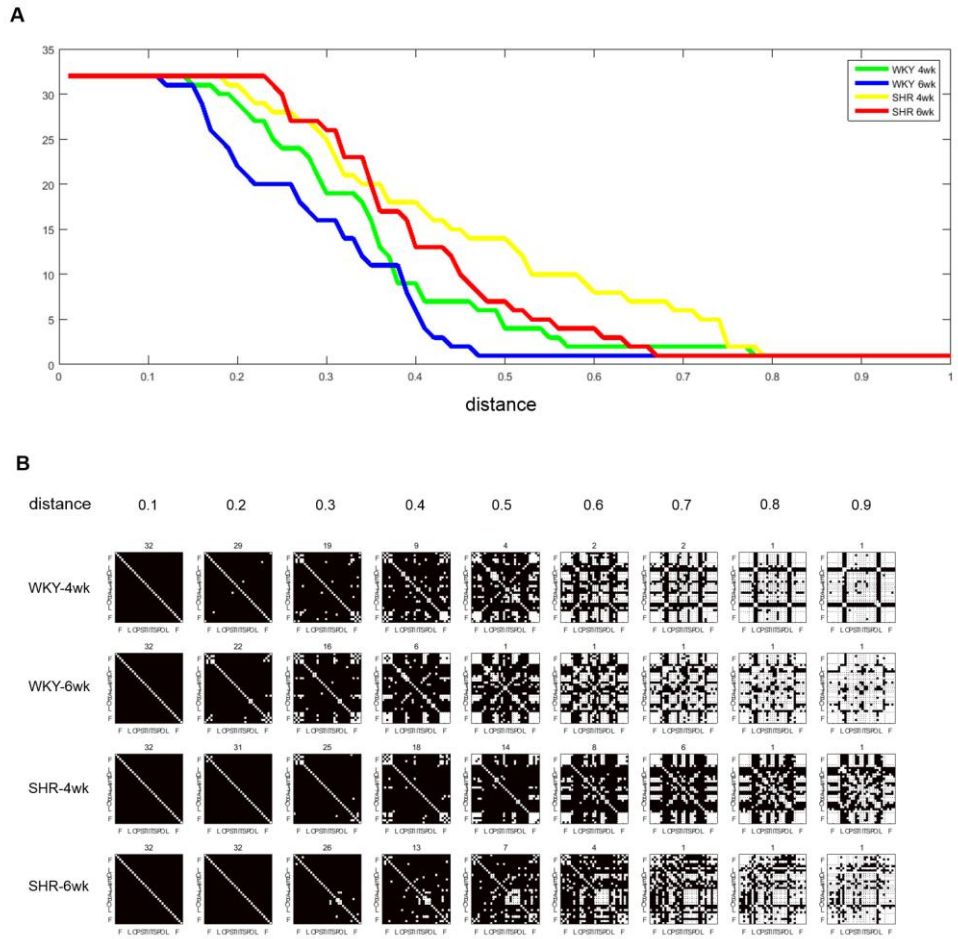

Figure 8. Graph filtration of the ADHD rat group and the normal control group at 4wk and 6wk ages

The barcodes of WKY-4wk, WKY-6wk, SHR-4wk, and SHR-6wk were displayed via graph filtration using filtration values, ε = 0.01, 0.02, …, 0.99 (A). The changes of metabolic networks with the filtration thresholds, ε = 0.1, 0.2, …, 0.9, were displayed for each group (B).

Difference of metabolic network in rat models

The metabolic connection between the limbic area (hippocampus) and other cortical/subcortical areas was significantly enhanced during maturation from 4wk-age to 6-wk age in the control group, WKY rats ($P < 0.05$, 10000 permutation) (Figure 9A). During the development of SHR ADHD rats from 4-wk age to 6-wk age, the interregional connections between another limbic area (Entorhinal cortex) to cerebral cortices were enhanced. Furthermore, the global enhancement of interregional connections was observed ($P < 0.05$, 10000 permutation) (Figure 9B). When comparing the SLMs of ADHD rats and control rats at the same 4-wk age, the ADHD group had significantly weaker bilateral interregional connections between entorhinal cortex and cerebral cortices ($P < 0.05$, 10000 permutations) (Figure 9C). When comparing the SLM of ADHD rats and control rats at the same 6-wk age, there was limited number of significantly weakened interregional connections in ADHD rats ($P < 0.05$, 10000 permutations) (Figure 9D). Also, there were weak connections between limbic to cortices with moderate significance ($P < 0.10$, 10000 permutations) (Figure 10). Meanwhile, the SLMs were not significantly different between the 6-wk aged ADHD rats and the 4-wk aged control rats except the interregional connections between bilateral thalamus (Figure 11). The single linkage dendrograms of the control rats and ADHD rats with 4-wk age and 6-wk age was illustrated in Figure 12.

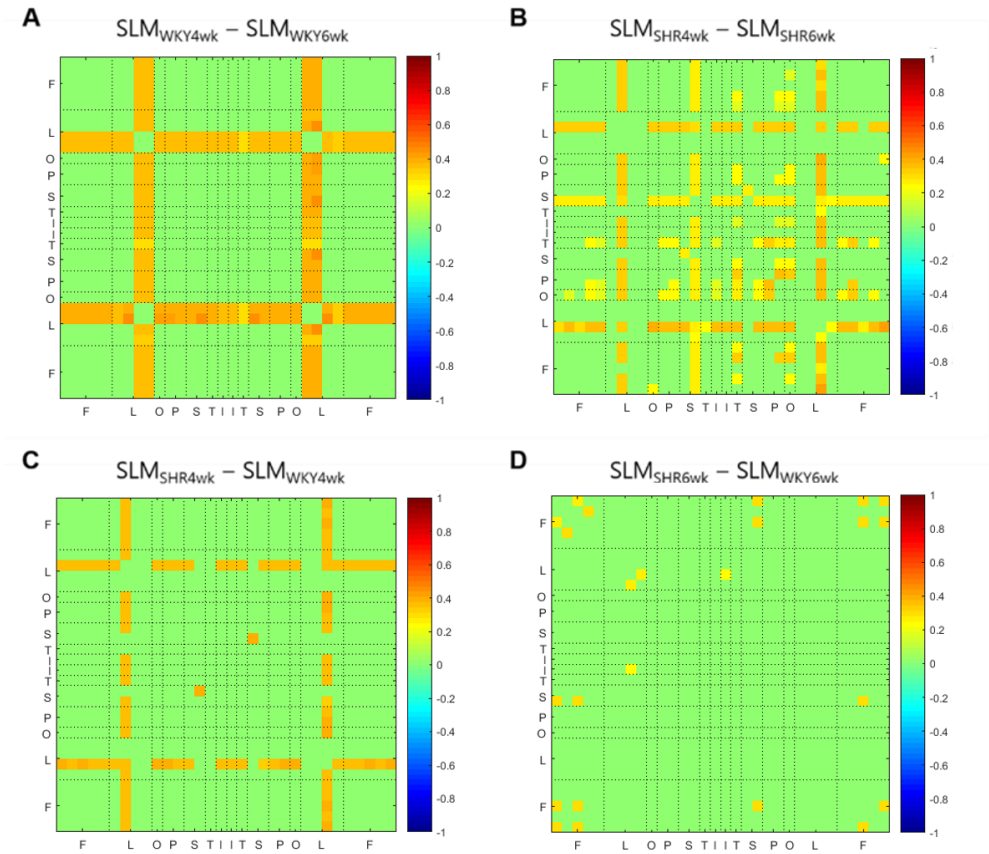

Figure 9. SLM difference with 10000-permuted test (P <0.05)

With the 10000-permuted test, statistically differed interregional connections between 32 ROIs were colored between WKY-4wk and WKY 6wk (A), between SHR-4wk and SHR-6wk (B), between SHR-4wk and WKY-4wk (C), and between SHR-6wk and WKY-6wk (D). Note: warm color, longer SLD; cold color, shorter SLD.

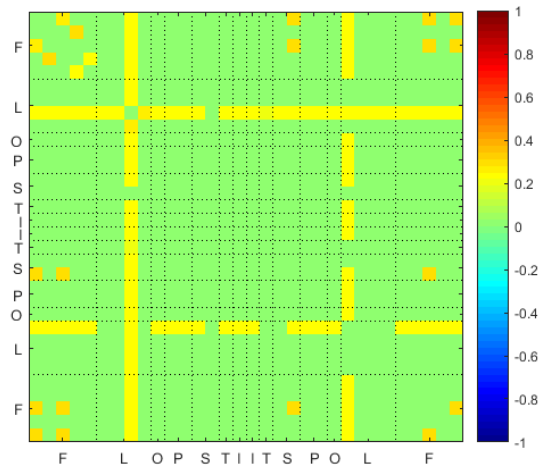

Figure 10. Difference of SLM between the SHR-6wk and the WKY-6wk with 10000 permutation test (P <0.10)

The SHR-6wk aged group showed a borderline significance of weak limbic (hippocampal)-cortical connections than the control rats with the same age.

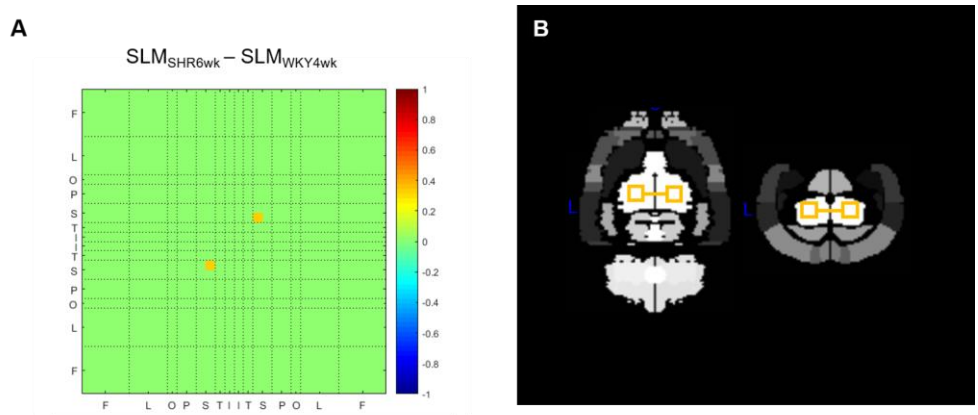

Figure 11. Comparison of SLM between SHR-6wk and WKY-4wk

ROIs with Significantly different SLD by the 10000-permuted test between SHR-6wk and WKY-4wk were visualized (P <0.05). Most connections between ROIs were not significantly different between SHR-6wk and WKY-4wk (A). The interthalamic connection (B) was significantly stronger in WKY-4wk compared to SHR-6wk. Abbreviations: ROI, region of interest; SHR, spontaneouly hypertensive rat; SLD, single linkage distance; SLM, single linkage matrix; WKY, Wistar Kyoto rat

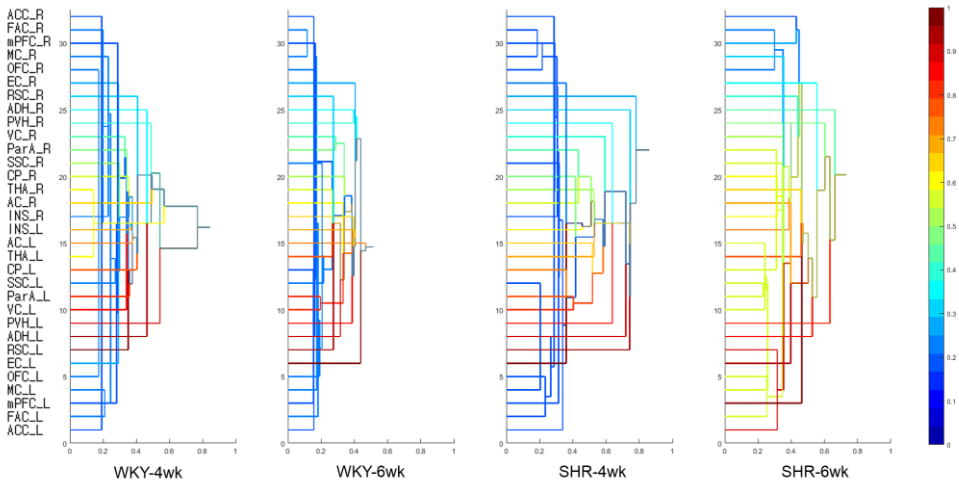

Figure 12. Single linkage dendrograms of rat brain metabolic networks

The x axis represented filtration values of distance. The y axis represented the ROIs of rat brain. The color of lines explained the distance from the giant component.

Modularization of brain network during development

The algorithmic displays following the Kamada and Kawai method of MST graphs were illustrated in figure 13 (48). The reward-motivation regions (caudoputamen [CP], mPFC and anterior cingulate cortex [ACC]) were colored as red, and the other reward system related regions were colored as green. The control rats showed well-modularization of the reward-motivation regions during development from 4-wk age to 6-wk age (Figure 13A-B). The ADHD 4-wk aged rats had the most segregated the reward-motivation regions (Figure 13C). During the development of the ADHD rats from 4-wk age to 6-wk age, the reward-motivation regions and reward-related regions start to construct the relatively modularized network. But the MST of ADHD 6-wk was still dissociated compared to the MST of control rats with the same age (Figure 13D). Circular plots of the MSTs of the control rats and the ADHD rats were illustrated in Figure 14.

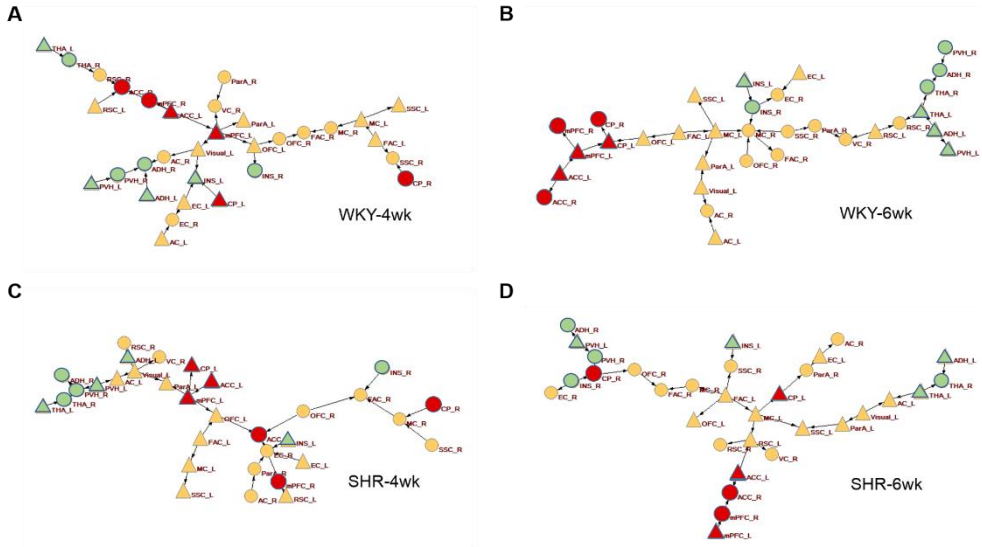

Figure 13. Minimum spanning tree of the control rats and ADHD rats

The MSTs of the control rat, WKY, and the ADHD rat, SHR were shown about 4-wk age and 6-wk age. The MST of WKY-4wk showed separate modularization of the reward-motivation regions, ACCs, mPFC, and CPs (A). The reward-motivation regions were modularized in the WKY-6wk group (B). The SHR-4wk group showed separation of the reward-motivation regions (C). Although the ACCs and mPFCs were modularized at 6wk-age for SHR, the less modularized state of CPs was sustained (D). Note: red-color, reward-motivation regions; green-color, reward-related regions; orange-color, other regions mainly cortices; triangle, left-side; circle, right-side.

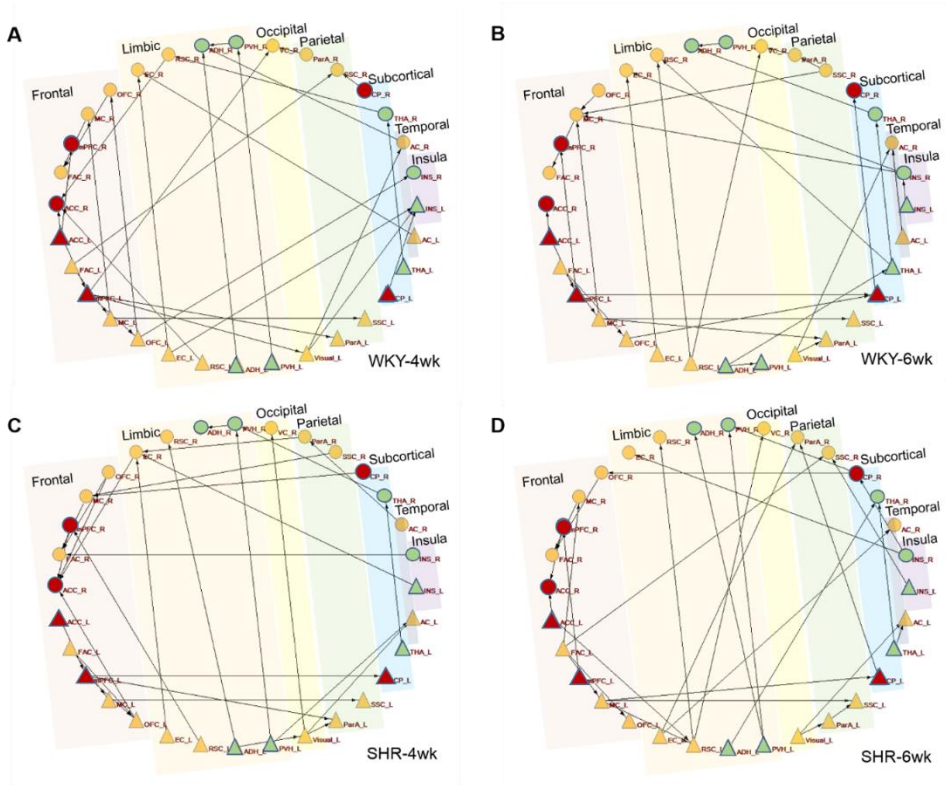

Figure 14. Circular plots of MSTs in the control rats and ADHD rats

The MSTs were visualized as circular plots for the rat groups of WKY-4wk (A), WKY-6wk (B), SHR-4wk (C), and SHR-6wk (D).

Part II. Brain functional network analysis in ADHD

Demographics of ADHD-200 cohort

Table 2 explained characteristics of the involved subjects from ADHD-200 cohort. There were 132 TDC subjects and 91 ADHD subjects. The TDC group (mean age, 11.3y ± 1.8y) is significantly younger than ADHD group (mean age, 11.9 ± 1.9) (P = 0.038). The ratio of male and female was significantly different between the TDC group (76:56, [58%:42%]) and ADHD group (82:9, [90%:10%]) (P <0.001). With the age criteria of 12 years-old, there were 85 subjects (64%) in $TDC_{8\text{-}12y}$ and 47 subjects (36%) in $TDC_{12\text{-}15y}$. There were 42 subjects (46%) of $ADHD_{8\text{-}12y}$ and 49 subjects (54%) of $ADHD_{12\text{-}15y}$. The ADHD index was significantly higher in the ADHD group (50.5 ± 8.1) than the TDC group (29.6 ± 6.5) (P <0.001). The IQ was significantly higher in the TDC group (106.1 ± 13.2) than the ADHD group (118.4 ± 13.3) (P <0.001). The medication naïve ratio in the ADHD group was 70%. When comparing the demographics of $ADHD_{8\text{-}12y}$ and $ADHD_{12\text{-}15y}$, there was no significant difference of the male ratio (86% vs. 94%, respectively), ADHD index (51.4 ± 8.1 vs. 49.8 ± 8.2, respectively), IQ (106.4 ± 14.8 vs. 105.8 ± 11.9, respectively), and the ratio of medication naïve (64% vs. 76%) (all P >0.05) (Table 3).

Table 2. Demographics of subjects from ADHD-200 cohort

	TDC (n = 132)	ADHD (n = 91)	P-value
Age (y)	11.3 ± 1.8	11.9 ± 1.9	0.038
8-12y	85 (64%)	42 (46%)	
12-15y	47 (36%)	49 (54%)	
Sex (M:F)	76:56 (58%:42%)	82:9 (90%:10%)	<0.001
ADHD-index†	29.6 ± 6.5	50.5 ± 8.1	<0.001
IQ‡	118.4 ± 13.3	106.1 ± 13.2	<0.001
Medication naive		64 (70%)	

†ADHD Rating Scale-IV (ADHD-RS)

‡Wechsler Intelligence Scale for Chinese Children-Revised (WISCC-R)

Note: Peking University data from ADHD-200

Table 3. Comparison of demographics of ADHD subjects (8-12y vs. 12-15y)

	ADHD, 8-12y (n = 42)	ADHD, 12-15y (n = 49)	P-value
Age (y)	10.1 ± 0.9	13.4 ± 0.7	
Sex (M:F)	36:6 (86%:14%)	46:3 (94%:6%)	0.193
ADHD-index†	51.4 ± 8.1	49.8 ± 8.2	0.389
IQ‡	106.4 ± 14.8	105.8 ± 11.9	0.842
Medication naive	27:15 (64%:36%)	37:12 (76%:24%)	0.243

†ADHD Rating Scale-IV (ADHD-RS)

‡Wechsler Intelligence Scale for Chinese Children-Revised (WISCC-R)

Note: Peking University data from ADHD-200

Construction of functional individual SLM

From the correlation matrix of each subject, distance matrix and SLM were sequentially obtained. Barcodes by persistent homology for all subjects were drawn for the groups of $TDC_{8\text{-}12y}$ (Figure 15A), $TDC_{12\text{-}15y}$ (Figure 15B), $ADHD_{8\text{-}12y}$ (Figure 15C), and $ADHD_{12\text{-}15y}$ (Figure 15D). The averages and 1 standard deviations of AUC-ROCs in the groups of $TDC_{8\text{-}12y}$, $TDC_{12\text{-}15y}$, $ADHD_{8\text{-}12y}$, and $ADHD_{12\text{-}15y}$ were 47.4 ± 2.9, 45.7 ± 2.8, 46.8 ± 2.4, and 45.9 ± 2.4, respectively. There was a significant difference of the average AUC-ROC of $TDC_{8\text{-}12y}$ compared to $TDC_{12\text{-}15y}$ and $ADHD_{12\text{-}15y}$ (all $P < 0.05$ in post-hoc analysis) (Figure 16).

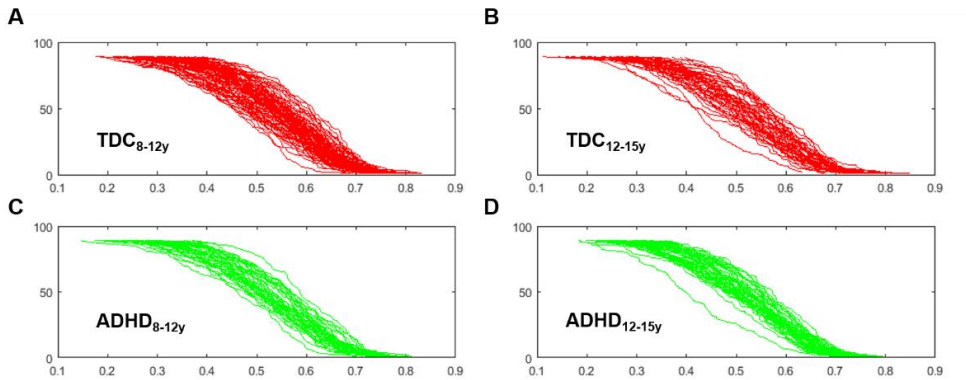

Figure 15. Barcodes of subjects in $TDC_{8\text{-}12y}$, $TDC_{12\text{-}15y}$, $ADHD_{8\text{-}12y}$, and $ADHD_{12\text{-}15y}$

Barcodes using persistent homology were displayed for all subjects in the groups of $TDC_{8\text{-}12y}$ (A), $TDC_{12\text{-}15y}$ (B), $ADHD_{8\text{-}12y}$ (C), and $ADHD_{12\text{-}15y}$ (D). Abbreviations: ADHD, attention deficit/hyperactivity disorder; TDC, typical developing control.

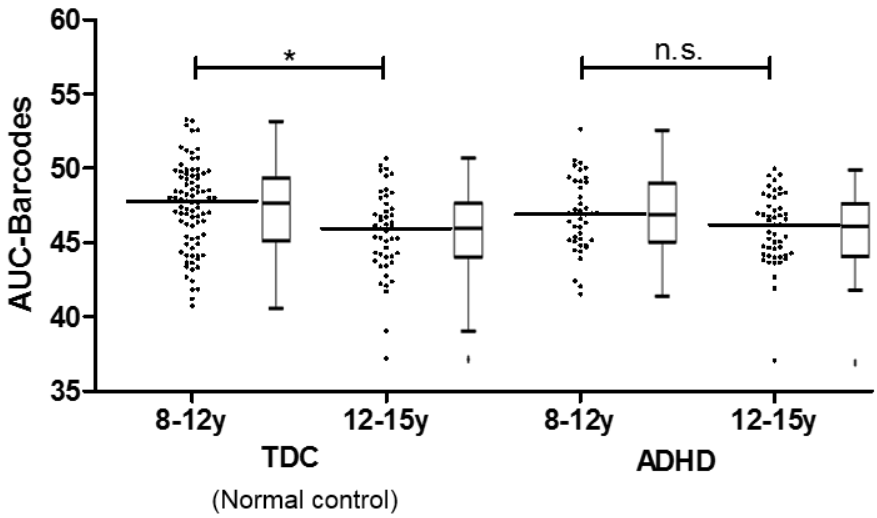

Figure 16. Comparison of area-under curves of barcodes for TDC and ADHD

Box and whisker plots with Tukey method were drawn for the AUCs of the barcodes of $TDC_{8\text{-}12y}$, $TDC_{12\text{-}15y}$, $ADHD_{8\text{-}12y}$, and $ADHD_{12\text{-}15y}$. Note: *, statistically significant. Abbreviations: ADHD, attention deficit/hyperactivity disorder; TDC, typical developing control.

Difference of interregional connections during development

To evaluate maturation of functional network, the rank-sum test was conducted for SLDs of all interregional connections between $TDC_{8\text{-}12y}$ and $TDC_{12\text{-}15y}$, and between $ADHD_{8\text{-}12y}$ and $ADHD_{12\text{-}15y}$. The $TDC_{12\text{-}15y}$ group showed a significant difference in functional network compared to the $TDC_{8\text{-}12y}$ group that globally faster construction of interregional functional connections including limbic-to-cortices (FDR <0.05) (Figure 17A). Meanwhile, the $ADHD_{12\text{-}15y}$ group had the significantly faster construction of interregional functional connections among limited cortices (FDR <0.05). However, there was no significant difference in interregional connections including limbic, occipital cortex, and subcortical regions between $ADHD_{8\text{-}12y}$ and $ADHD_{12\text{-}15y}$ groups (FDR >0.05) (Figure 17B). No difference of SLDs in the 90 ROIs was observed between networks of $TDC_{8\text{-}12y}$ and $ADHD_{8\text{-}12y}$ (Figure 17C). Meanwhile, $TDC_{8\text{-}12y}$ had significantly increased the interregional connection between right putamen and right insula than $ADHD_{8\text{-}12y}$ (FDR <0.05) (Figure 17D).

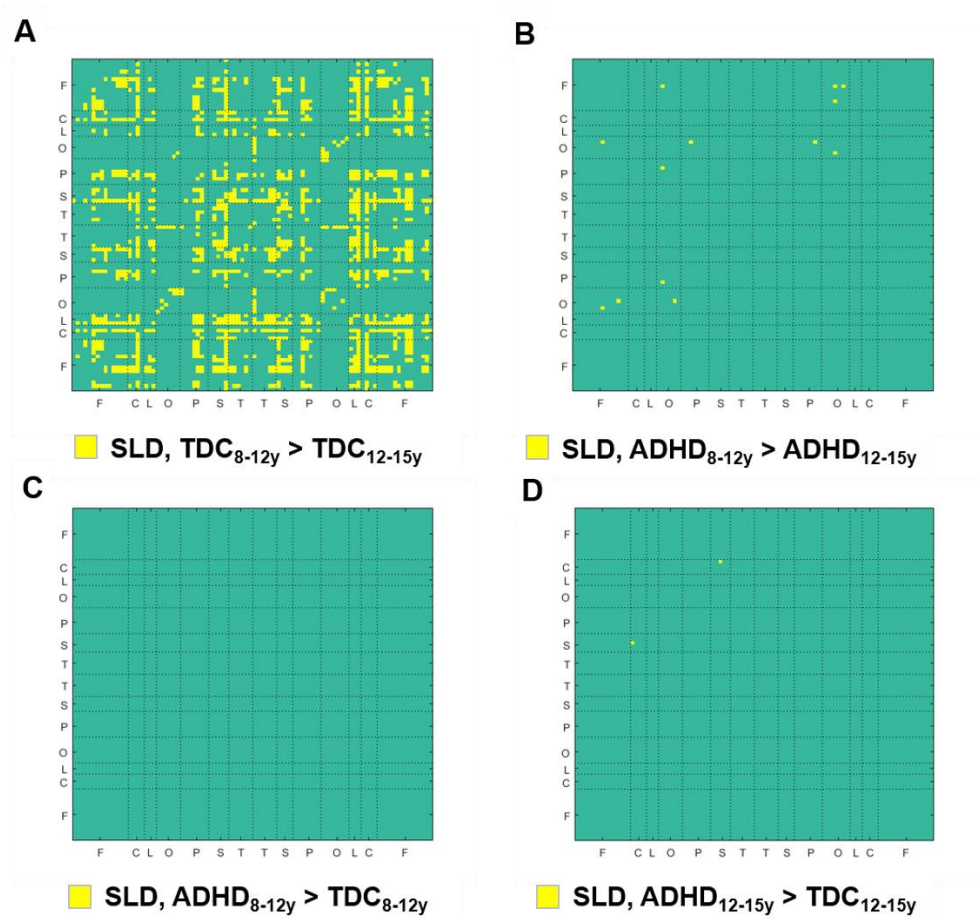

Figure 17. Comparison of SLDs among $TDC_{8\text{-}12y}$, $TDC_{12\text{-}15y}$, $ADHD_{8\text{-}12y}$, and $ADHD_{12\text{-}15y}$

The significantly enforced interregional functional connections during grow-up to adolescent was displayed for TDCs (A) and ADHD-patients (B). No difference of SLDs between $ADHD_{8\text{-}12y}$ and $TDC_{8\text{-}12y}$ was observed (C). The interregional connection between right putamen and right insula was increased in $TDC_{12\text{-}15y}$ than $ADHD_{12\text{-}15y}$ (D). Note: statistical significance, FDR <0.05. Abbreviations: ADHD, attention deficit/hyperactivity disorder; TDC, typical developing control; SLD, single linkage distance.

Part III. Maturation of metabolic network based on volume entropy

Change of volume entropy during maturations in rat models

Volume entropy was calculated for each rat group with 4wk and 6wk ages using the distance matrices with every available threshold. Higher volume entropy was observed in the control rats compared to the ADHD rats. There was a trend of increasing volume entropy during maturation from 4wk to 6wk in both groups, but more enhanced in the control rats. The highest volume entropy was observed in the WKY-6wk group. The volume entropy of WKY-4wk group with thresholds of 0.8~0.9 was higher than that of SHR-6wk group. When allowing distance around 1.0, the volume entropy of WKY-4wk group was similar to that of SHR-6wk group. The SHR-4wk always had the lowest volume entropy compared to other groups (Figure 18).

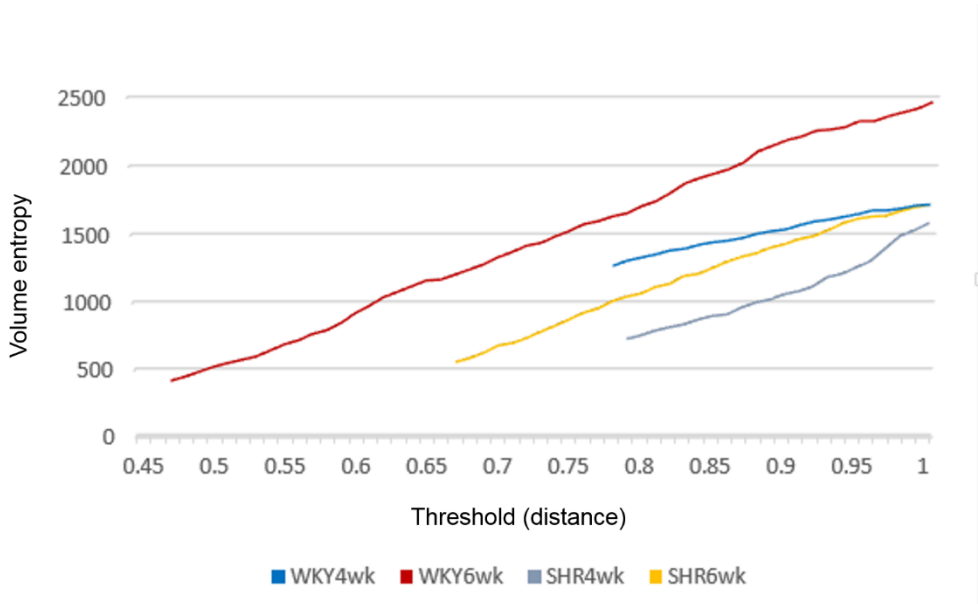

Figure 18. Volume entropy with varying thresholds on rat metabolic network

Volume entropy changes with varying thresholds were displayed for WKY-4wk, WKY-6wk, SHR-4wk, and SHR-6wk.

Comparison of volume entropy in human fMRI data

Volume entropy was calculated for all TDC and ADHD patients included in this study. There was a significant weak positive correlation between age and volume entropy in the TDC group (r, 0.240; P = 0.006) (Figure 19A). However, no significant correlation was observed in the ADHD group (P >0.05) (Figure 19B). The $TDC_{12\text{-}15y}$ group ($1.942 \times 10^4 \pm 398$) had significantly higher volume entropy compared to the $TDC_{8\text{-}12y}$ group ($1.919 \times 10^4 \pm 363$; P <0.05 in post-hoc analysis). No further significant difference was observed between the TDC and ADHD groups (Figure 20).

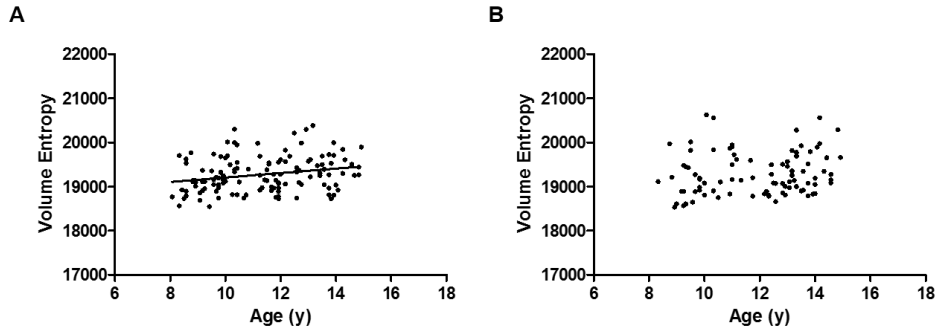

Figure 19. Correlation plot between age and individual volume entropy

The positive correlation between age and volume entropy was significant in the TDC group (A). Age and volume entropy was not correlated to each other in the ADHD group (B).

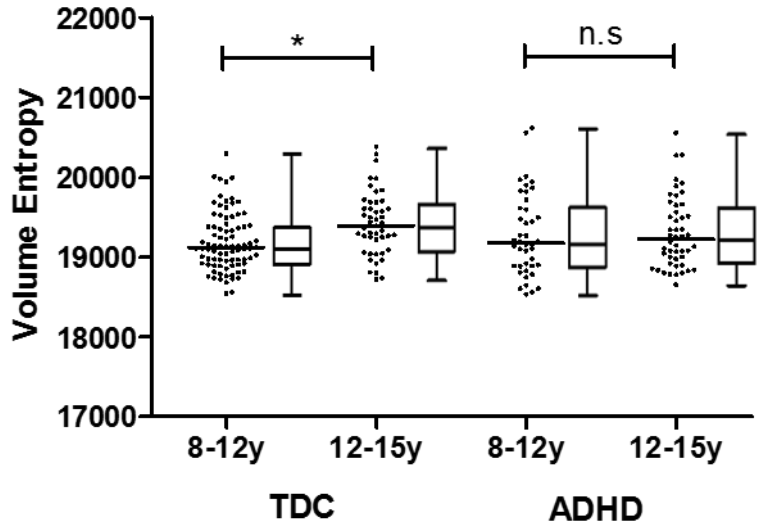

Figure 20. Comparison of functional individual volume entropy in TDC and ADHD during development

Volume entropies were compared among $TDC_{8\text{-}12y}$, $TDC_{12\text{-}15y}$, $ADHD_{8\text{-}12y}$, and $ADHD_{12\text{-}15y}$ by an ANOVA test with a post-hoc analysis. After maturation, TDC had higher volume entropy. Note: *, P-value <0.05; n.s, non-significant.

Discussion

Brain network analysis is a promising approach to explain complex brain developmental disorders like ADHD. The preclinical experiment using paired repetitive ^{18}F-FDG PET imaging about metabolic network analyzed by persistent homology provided the strong evidence of delayed maturation of limbic-cortical interregional connections in ADHD during grow-up from childhood (4wk-age) to entry of adolescent (6wk-age). The reward-motivation regions were modulated during development in the controls, but less modularized in the ADHD rats during development to 6wk-age. The functional network analysis using persistent homology in the clinical data showed a global strengthening of interregional connections from childhood to adolescent in the TDC group. On the contrary, the global reinforcement of interregional connections was not found in the ADHD group. Nonetheless, only limited interregional connections were significantly different between the $TDC_{12\text{-}15y}$ and $ADHD_{12\text{-}15y}$. The volume entropy change with varying filtration showed the higher efficiency of information flow in the normal network compared to the ADHD network, and in the matured network compared to the less matured network. Increasing volume entropy during grow-up in the TDC group and not in the ADHD group explained maturation of brain network in TDC and maturation disturbance in ADHD based on the efficiency of information flow on a network.

In a comparison of DMN in TDC at early school age (7-9 years old) and normal adults by a previous study, young TDC had a sparse functional connection. In contrast, the cohesively interconnected network was identified in normal adults. The main difference between young TDC and adults were anteroposterior functional connections in the midline of DMN (49). Similar findings that increased connectivity between the anterior and posterior parts of DMN and sensory-motor cortices during maturation were reported according to in comparison of the metabolic network

among normal adolescent rats of 5wk, 10wk, and 15wk aged (50). Meanwhile, the present preclinical result in this study suggested increased metabolic connectivity of hippocampal to all cortical regions during maturation of 4wk to 6wk aged. In the present clinical analysis, increased functional connectivity among global regions was observed during maturation from childhood to adolescent. Additionally, it seemed that during development, brain network normally evolved to have more efficiency in information processing according to the volume entropy comparison results.

There has been controversy as to whether ADHD is caused by delays in brain development or, in part, deviation from typical brain development (30). Previous work has found evidence of delayed maturation in ADHD regarding cortical thickness, which showed that the delay of cortical maturation was observed in most of the cerebrum, and the most prominent area was the prefrontal area (28). Recently, a mega-analysis about subcortical structural alteration based on T1-weighted MR imaging including 1713 patients with ADHD and 1529 controls from 23 sites has supported the hypothesis of delayed brain maturation in ADHD (12). According to the report, ADHD involves reduction of the volume of subcortical regions which were amygdala, caudate, hippocampus, putamen, and nucleus accumbens compared to control, and the difference of volumes was highest in children's brain. There has been supporting delayed maturation based on not only for structural alteration but also for functional connectivity, especially in DMN. In particular, delays in ADHD were observed not only in the midline of the DMN but also in the DMN connection with the right lateralized prefrontal region (frontoparietal network) and anterior insula (ventral attention network) (51).

Our preclinical result had strengths in observing maturation of the brain metabolic network in the same subjects. Noteworthy, in our present metabolic network analysis in SHR model, the delayed maturation of cortical connection to the limbic region

was identified compared to WKY control. This result was a concordant result to the previous clinical results of structural alteration in cortical thickness and subcortical regions. Also, there has been a concordant result to our metabolic network analysis from a preclinical study using resting-state fMRI imaging in another rat ADHD model, Naples-High-Excitability (NHE) rat, which showed decreased connectivity between the hippocampus and all cortex, even though information of rat-age was not provided (52). Meanwhile, there has been a preclinical study using fMRI in 6wk-old SHR model to investigate variations in the DMN under different dose of isoflurane anesthesia. The preclinical study showed that there was a major difference of activities in hippocampal and caudate-putamen regions (53).

Regardless of that this fMRI data of childhood and adolescent were not obtained from same subjects, our clinical result about functional network also supported the difference of brain maturation between ADHD and TDC. Not like global enforcement of functional connections in TDC, ADHD showed limited enforcement of interregional connections between frontal, parietal, and temporal cortices during maturation from childhood to adolescent. However, the connection including subcortical regions did not show any significant difference. Volume entropy explained that ADHD-adolescent did not differ to ADHD-childhood in information processing efficiency but significantly decreased than that in TDC-adolescent.

Conclusions

The maturation of brain network from childhood to adolescent was normally observed mainly as increased limbic-cortical connections in preclinical metabolic connectivity and as increased global connections in functional connectivity in typically developing children. Increased volume entropy during grow-up was revealed as another evidence of brain maturation supported by both preclinical and human data analysis. The ADHD rats showed the prominent delayed maturation of metabolic network in limbic-cortical connections. The human functional network analysis showed the disturbance of brain maturation related to ADHD by persistent homology and volume entropy. The results of this study partly support the hypothesis that delayed brain maturation in ADHD and gave robust insight into brain developments in ADHD.

Acknowledgments

This work was supported by the National Research Foundation of Korea(NRF) grant funded by the Korea government(MSIP) (2015M3C7A1028926). The preprocessed human ADHD and TDC fMRI data used in this article were obtained from the ADHD-200 database (http://fcon_1000.projects.nitrc.org/indi/adhd200/).

Conflict of interest

Nothing to declare.

References

1. Tarver J, Daley D, Sayal K. Attention-deficit hyperactivity disorder (ADHD): an updated review of the essential facts. Child: care, health and development. 2014;40(6):762-74.

2. Polanczyk G, de Lima MS, Horta BL, Biederman J, Rohde LA. The worldwide prevalence of ADHD: a systematic review and metaregression analysis. The American journal of psychiatry. 2007;164(6):942-8.

3. Increasing prevalence of parent-reported attention-deficit/hyperactivity disorder among children --- United States, 2003 and 2007. MMWR Morbidity and mortality weekly report. 2010;59(44):1439-43.

4. Barkley RA, Fischer M, Smallish L, Fletcher K. The persistence of attention-deficit/hyperactivity disorder into young adulthood as a function of reporting source and definition of disorder. Journal of abnormal psychology. 2002;111(2):279-89.

5. Biederman J, Monuteaux MC, Mick E, Spencer T, Wilens TE, Silva JM, et al. Young adult outcome of attention deficit hyperactivity disorder: a controlled 10-year follow-up study. Psychological medicine. 2006;36(2):167-79.

6. Wilens TE, Faraone SV, Biederman J. Attention-deficit/hyperactivity disorder in adults. Jama. 2004;292(5):619-23.

7. Kessler RC, Adler L, Ames M, Barkley RA, Birnbaum H, Greenberg P, et al. The prevalence and effects of adult attention deficit/hyperactivity disorder on work performance in a nationally representative sample of workers. Journal of occupational and environmental medicine. 2005;47(6):565-72.

8. Biederman J, Faraone SV, Spencer TJ, Mick E, Monuteaux MC, Aleardi M. Functional impairments in adults with self-reports of diagnosed ADHD: A controlled study of 1001 adults in the community. The Journal of clinical psychiatry. 2006;67(4):524-40.

9. Goldman LS, Genel M, Bezman RJ, Slanetz PJ. Diagnosis and treatment of attention-deficit/hyperactivity disorder in children and adolescents. Jama. 1998;279(14):1100-7.

10. Zhang L, Chang S, Li Z, Zhang K, Du Y, Ott J, et al. ADHDgene: a genetic database for attention deficit hyperactivity disorder. Nucleic acids research.

2012;40(Database issue):D1003-9.
11. Banerjee TD, Middleton F, Faraone SV. Environmental risk factors for attention-deficit hyperactivity disorder. Acta paediatrica. 2007;96(9):1269-74.
12. Hoogman M, Bralten J, Hibar DP, Mennes M, Zwiers MP, Schweren LSJ, et al. Subcortical brain volume differences in participants with attention deficit hyperactivity disorder in children and adults: a cross-sectional mega-analysis. The lancet Psychiatry. 2017;4(4):310-9.
13. Cubillo A, Halari R, Smith A, Taylor E, Rubia K. A review of fronto-striatal and fronto-cortical brain abnormalities in children and adults with Attention Deficit Hyperactivity Disorder (ADHD) and new evidence for dysfunction in adults with ADHD during motivation and attention. Cortex; a journal devoted to the study of the nervous system and behavior. 2012;48(2):194-215.
14. Castellanos FX, Sonuga-Barke EJ, Milham MP, Tannock R. Characterizing cognition in ADHD: beyond executive dysfunction. Trends in cognitive sciences. 2006;10(3):117-23.
15. Dickstein SG, Bannon K, Castellanos FX, Milham MP. The neural correlates of attention deficit hyperactivity disorder: an ALE meta-analysis. Journal of child psychology and psychiatry, and allied disciplines. 2006;47(10):1051-62.
16. Rubia K. "Cool" inferior frontostriatal dysfunction in attention-deficit/hyperactivity disorder versus "hot" ventromedial orbitofrontal-limbic dysfunction in conduct disorder: a review. Biological psychiatry. 2011;69(12):e69-87.
17. Metin B, Krebs RM, Wiersema JR, Verguts T, Gasthuys R, van der Meere JJ, et al. Dysfunctional modulation of default mode network activity in attention-deficit/hyperactivity disorder. Journal of abnormal psychology. 2015;124(1):208-14.
18. Sonuga-Barke EJ, Castellanos FX. Spontaneous attentional fluctuations in impaired states and pathological conditions: a neurobiological hypothesis. Neuroscience and biobehavioral reviews. 2007;31(7):977-86.
19. Castellanos FX, Margulies DS, Kelly C, Uddin LQ, Ghaffari M, Kirsch A, et al. Cingulate-precuneus interactions: a new locus of dysfunction in adult attention-deficit/hyperactivity disorder. Biological psychiatry. 2008;63(3):332-7.
20. Fassbender C, Zhang H, Buzy WM, Cortes CR, Mizuiri D, Beckett L, et al. A lack of default network suppression is linked to increased distractibility in ADHD.

Brain research. 2009;1273:114-28.
21. Buckner RL, Andrews-Hanna JR, Schacter DL. The brain's default network: anatomy, function, and relevance to disease. Annals of the New York Academy of Sciences. 2008;1124:1-38.
22. Castellanos FX, Proal E. Large-scale brain systems in ADHD: beyond the prefrontal-striatal model. Trends in cognitive sciences. 2012;16(1):17-26.
23. Stevens MC, Pearlson GD, Kiehl KA. An FMRI auditory oddball study of combined-subtype attention deficit hyperactivity disorder. The American journal of psychiatry. 2007;164(11):1737-49.
24. Rubia K, Cubillo A, Smith AB, Woolley J, Heyman I, Brammer MJ. Disorder-specific dysfunction in right inferior prefrontal cortex during two inhibition tasks in boys with attention-deficit hyperactivity disorder compared to boys with obsessive-compulsive disorder. Human brain mapping. 2010;31(2):287-99.
25. Peterson BS, Potenza MN, Wang Z, Zhu H, Martin A, Marsh R, et al. An FMRI study of the effects of psychostimulants on default-mode processing during Stroop task performance in youths with ADHD. The American journal of psychiatry. 2009;166(11):1286-94.
26. Edin F, Klingberg T, Stodberg T, Tegner J. Fronto-parietal connection asymmetry regulates working memory distractibility. Journal of integrative neuroscience. 2007;6(4):567-96.
27. Neufang S, Fink GR, Herpertz-Dahlmann B, Willmes K, Konrad K. Developmental changes in neural activation and psychophysiological interaction patterns of brain regions associated with interference control and time perception. NeuroImage. 2008;43(2):399-409.
28. Shaw P, Eckstrand K, Sharp W, Blumenthal J, Lerch JP, Greenstein D, et al. Attention-deficit/hyperactivity disorder is characterized by a delay in cortical maturation. Proceedings of the National Academy of Sciences of the United States of America. 2007;104(49):19649-54.
29. Shaw P, Lerch J, Greenstein D, Sharp W, Clasen L, Evans A, et al. Longitudinal mapping of cortical thickness and clinical outcome in children and adolescents with attention-deficit/hyperactivity disorder. Archives of general psychiatry. 2006;63(5):540-9.
30. Shaw P, Rabin C. New insights into attention-deficit/hyperactivity disorder

using structural neuroimaging. Current psychiatry reports. 2009;11(5):393-8.
31. Sontag TA, Tucha O, Walitza S, Lange KW. Animal models of attention deficit/hyperactivity disorder (ADHD): a critical review. ADHD Attention Deficit and Hyperactivity Disorders. 2010;2(1):1-20.
32. Fornito A, Zalesky A, Bullmore E. Fundamentals of brain network analysis: Academic Press; 2016.
33. Lichtman JW, Denk W. The big and the small: challenges of imaging the brain's circuits. Science (New York, NY). 2011;334(6056):618-23.
34. Niven JE, Laughlin SB. Energy limitation as a selective pressure on the evolution of sensory systems. The Journal of experimental biology. 2008;211(Pt 11):1792-804.
35. van den Heuvel MP, Hulshoff Pol HE. Exploring the brain network: a review on resting-state fMRI functional connectivity. European neuropsychopharmacology : the journal of the European College of Neuropsychopharmacology. 2010;20(8):519-34.
36. Bota M, Sporns O, Swanson LW. Architecture of the cerebral cortical association connectome underlying cognition. Proceedings of the National Academy of Sciences of the United States of America. 2015;112(16):E2093-101.
37. Markov NT, Ercsey-Ravasz M, Lamy C, Ribeiro Gomes AR, Magrou L, Misery P, et al. The role of long-range connections on the specificity of the macaque interareal cortical network. Proceedings of the National Academy of Sciences of the United States of America. 2013;110(13):5187-92.
38. Bullmore E, Sporns O. Complex brain networks: graph theoretical analysis of structural and functional systems. Nature reviews Neuroscience. 2009;10(3):186-98.
39. Bassett DS, Nelson BG, Mueller BA, Camchong J, Lim KO. Altered resting state complexity in schizophrenia. NeuroImage. 2012;59(3):2196-207.
40. Lee H, Kang H, Chung MK, Kim BN, Lee DS. Persistent brain network homology from the perspective of dendrogram. IEEE transactions on medical imaging. 2012;31(12):2267-77.
41. Hahm J, Lee H, Park H, Kang E, Kim YK, Chung CK, et al. Gating of memory encoding of time-delayed cross-frequency MEG networks revealed by graph filtration based on persistent homology. Scientific reports. 2017;7:41592.

42. Kim E, Kang H, Lee H, Lee HJ, Suh MW, Song JJ, et al. Morphological brain network assessed using graph theory and network filtration in deaf adults. Hearing research. 2014;315:88-98.
43. Im HJ, Hahm J, Kang H, Choi H, Lee H, Hwang do W, et al. Disrupted brain metabolic connectivity in a 6-OHDA-induced mouse model of Parkinson's disease examined using persistent homology-based analysis. Scientific reports. 2016;6:33875.
44. Sagvolden T, Johansen EB, Woien G, Walaas SI, Storm-Mathisen J, Bergersen LH, et al. The spontaneously hypertensive rat model of ADHD--the importance of selecting the appropriate reference strain. Neuropharmacology. 2009;57(7-8):619-26.
45. Sengupta P. The Laboratory Rat: Relating Its Age With Human's. International journal of preventive medicine. 2013;4(6):624-30.
46. Schiffer WK, Mirrione MM, Biegon A, Alexoff DL, Patel V, Dewey SL. Serial microPET measures of the metabolic reaction to a microdialysis probe implant. Journal of neuroscience methods. 2006;155(2):272-84.
47. Chen Z, Dehmer M, Emmert-Streib F, Shi Y. Entropy of Weighted Graphs with Randi c Weights. Entropy. 2015;17(6):3710-23.
48. Kamada T, Kawai S. An algorithm for drawing general undirected graphs. Information processing letters. 1989;31(1):7-15.
49. Fair DA, Cohen AL, Dosenbach NU, Church JA, Miezin FM, Barch DM, et al. The maturing architecture of the brain's default network. Proceedings of the National Academy of Sciences of the United States of America. 2008;105(10):4028-32.
50. Choi H, Choi Y, Kim KW, Kang H, Hwang DW, Kim EE, et al. Maturation of metabolic connectivity of the adolescent rat brain. eLife. 2015;4.
51. Sripada CS, Kessler D, Angstadt M. Lag in maturation of the brain's intrinsic functional architecture in attention-deficit/hyperactivity disorder. Proceedings of the National Academy of Sciences of the United States of America. 2014;111(39):14259-64.
52. Zoratto F, Palombelli GM, Ruocco LA, Carboni E, Laviola G, Sadile AG, et al. Enhanced limbic/impaired cortical-loop connection onto the hippocampus of NHE rats: Application of resting-state functional connectivity in a preclinical ADHD

model. Behavioural brain research. 2017;333:171-8.
53. Huang SM, Wu YL, Peng SL, Peng HH, Huang TY, Ho KC, et al. Inter-Strain Differences in Default Mode Network: A Resting State fMRI Study on Spontaneously Hypertensive Rat and Wistar Kyoto Rat. Scientific reports. 2016;6:21697.

Supplemental table 1. Analyzed ROIs on the rat template (Schiffer)

No	Full name	Abbreviations	Location	Rt/Lt
1	Anterior Cortex Cingulate Rt	ACC_R	Frontal	Rt
2	Cortex Frontal Association Rt	FAC_R	Frontal	Rt
3	Cortex Medial Prefrontal Rt	mPFC_R	Frontal	Rt
4	Cortex Motor Rt	MC_R	Frontal	Rt
5	Cortex Orbitofrontal Rt	OFC_R	Frontal	Rt
6	Cortex Entorhinal Rt	EC_R	Limbic	Rt
7	Cortex Retrosplenial Rt	RSC_R	Limbic	Rt
8	Hippocampus Antero Dorsal Rt	ADH_R	Limbic	Rt
9	Hippocampus Posterior Rt	PVH_R	Limbic	Rt
10	Cortex Visual Rt	VC_R	Occipital	Rt
11	Cortex Par A Rt	ParA_R	Parietal	Rt
12	Cortex Somatosensory Rt	SSC_R	Parietal	Rt
13	Caudate Putamen Rt	CP_R	Subcortical	Rt
14	Thalamus Whole Rt	THA_R	Subcortical	Rt
15	Cortex Auditory Rt	AC_R	Temporal	Rt
16	Cortex Insular Rt	INS_R	Insula	Rt
17	Cortex Insular Lt	INS_L	Insula	Lt
18	Cortex Auditory Lt	AC_L	Temporal	Lt
19	Thalamus Whole Lt	THA_L	Subcortical	Lt
20	Caudate Putamen Lt	CP_L	Subcortical	Lt
21	Cortex Somatosensory Lt	SSC_L	Parietal	Lt
22	Cortex Par A Lt	ParA_L	Parietal	Lt
23	Cortex Visual Lt	VC_L	Occipital	Lt
24	Hippocampus Posterior Lt	PVH_L	Limbic	Lt
25	Hippocampus Antero Dorsal Lt	ADH_L	Limbic	Lt
26	Cortex Retrosplenial Lt	RSC_L	Limbic	Lt
27	Cortex Entorhinal Lt	EC_L	Limbic	Lt
28	Cortex Orbitofrontal Lt	OFC_L	Frontal	Lt
29	Cortex Motor Lt	MC_L	Frontal	Lt
30	Cortex Medial Prefrontal Lt	mPFC_L	Frontal	Lt
31	Cortex Frontal Association Lt	FAC_L	Frontal	Lt
32	Anterior Cortex Cingulate Lt	ACC_L	Frontal	Lt

Supplemental table 2. Analyzed ROIs on the human AAL template

No	Full name	Abbreviations	Location	Rt/Lt
1	Precentral_R	PreCG.R	Frontal	Rt
2	Frontal_Sup_R	SFGdor.R	Frontal	Rt
3	Frontal_Sup_Orb_R	ORBsup.R	Frontal	Rt
4	Frontal_Mid_R	MFG.R	Frontal	Rt
5	Frontal_Mid_Orb_R	ORBmid.R	Frontal	Rt
6	Frontal_Inf_Oper_R	IFGoperc.R	Frontal	Rt
7	Frontal_Inf_Tri_R	IFGtriang.R	Frontal	Rt
8	Frontal_Inf_Orb_R	ORBinf.R	Frontal	Rt
9	Rolandic_Oper_R	ROL.R	Frontal	Rt
10	Supp_Motor_Area_R	SMA.R	Frontal	Rt
11	Olfactory_R	OLF.R	Frontal	Rt
12	Frontal_Sup_Medial_R	SFGmed.R	Frontal	Rt
13	Frontal_Med_Orb_R	ORBsupmed.R	Frontal	Rt
14	Rectus_R	REC.R	Frontal	Rt
15	Insula_R	INS.R	Cingulate_Insula	Rt
16	Cingulum_Ant_R	ACG.R	Cingulate_Insula	Rt
17	Cingulum_Mid_R	DCG.R	Cingulate_Insula	Rt
18	Cingulum_Post_R	PCG.R	Cingulate_Insula	Rt
19	Hippocampus_R	HIP.R	Limbic	Rt
20	ParaHippocampal_R	PHG.R	Limbic	Rt
21	Amygdala_R	AMYG.R	Limbic	Rt
22	Calcarine_R	CAL.R	Occipital	Rt
23	Cuneus_R	CUN.R	Occipital	Rt
24	Lingual_R	LING.R	Occipital	Rt
25	Occipital_Sup_R	SOG.R	Occipital	Rt
26	Occipital_Mid_R	MOG.R	Occipital	Rt
27	Occipital_Inf_R	IOG.R	Occipital	Rt
28	Fusiform_R	FFG.R	Temporal	Rt
29	Postcentral_R	PoCG.R	Parietal	Rt
30	Parietal_Sup_R	SPG.R	Parietal	Rt
31	Parietal_Inf_R	IPL.R	Parietal	Rt
32	SupraMarginal_R	SMG.R	Parietal	Rt
33	Angular_R	ANG.R	Parietal	Rt
34	Precuneus_R	PCUN.R	Parietal	Rt
35	Paracentral_Lobule_R	PCL.R	Frontal	Rt
36	Caudate_R	CAU.R	Subcortical	Rt
37	Putamen_R	PUT.R	Subcortical	Rt
38	Pallidum_R	PAL.R	Subcortical	Rt
39	Thalamus_R	THA.R	Subcortical	Rt
40	Heschl_R	HES.R	Temporal	Rt
41	Temporal_Sup_R	STG.R	Temporal	Rt
42	Temporal_Pole_Sup_R	TPOsup.R	Temporal	Rt
43	Temporal_Mid_R	MTG.R	Temporal	Rt
44	Temporal_Pole_Mid_R	TPOmid.R	Temporal	Rt
45	Temporal_Inf_R	ITG.R	Temporal	Rt
46	Temporal_Inf_L	ITG.L	Temporal	Lt

47	Temporal_Pole_Mid_L	TPOmid.L	Temporal	Lt
48	Temporal_Mid_L	MTG.L	Temporal	Lt
49	Temporal_Pole_Sup_L	TPOsup.L	Temporal	Lt
50	Temporal_Sup_L	STG.L	Temporal	Lt
51	Heschl_L	HES.L	Temporal	Lt
52	Thalamus_L	THA.L	Subcortical	Lt
53	Pallidum_L	PAL.L	Subcortical	Lt
54	Putamen_L	PUT.L	Subcortical	Lt
55	Caudate_L	CAU.L	Subcortical	Lt
56	Paracentral_Lobule_L	PCL.L	Frontal	Lt
57	Precuneus_L	PCUN.L	Parietal	Lt
58	Angular_L	ANG.L	Parietal	Lt
59	SupraMarginal_L	SMG.L	Parietal	Lt
60	Parietal_Inf_L	IPL.L	Parietal	Lt
61	Parietal_Sup_L	SPG.L	Parietal	Lt
62	Postcentral_L	PoCG.L	Parietal	Lt
63	Fusiform_L	FFG.L	Temporal	Lt
64	Occipital_Inf_L	IOG.L	Occipital	Lt
65	Occipital_Mid_L	MOG.L	Occipital	Lt
66	Occipital_Sup_L	SOG.L	Occipital	Lt
67	Lingual_L	LING.L	Occipital	Lt
68	Cuneus_L	CUN.L	Occipital	Lt
69	Calcarine_L	CAL.L	Occipital	Lt
70	Amygdala_L	AMYG.L	Limbic	Lt
71	ParaHippocampal_L	PHG.L	Limbic	Lt
72	Hippocampus_L	HIP.L	Limbic	Lt
73	Cingulum_Post_L	PCG.L	Cingulate_Insula	Lt
74	Cingulum_Mid_L	DCG.L	Cingulate_Insula	Lt
75	Cingulum_Ant_L	ACG.L	Cingulate_Insula	Lt
76	Insula_L	INS.L	Cingulate_Insula	Lt
77	Rectus_L	REC.L	Frontal	Lt
78	Frontal_Med_Orb_L	ORBsupmed.L	Frontal	Lt
79	Frontal_Sup_Medial_L	SFGmed.L	Frontal	Lt
80	Olfactory_L	OLF.L	Frontal	Lt
81	Supp_Motor_Area_L	SMA.L	Frontal	Lt
82	Rolandic_Oper_L	ROL.L	Frontal	Lt
83	Frontal_Inf_Orb_L	ORBinf.L	Frontal	Lt
84	Frontal_Inf_Tri_L	IFGtriang.L	Frontal	Lt
85	Frontal_Inf_Oper_L	IFGoperc.L	Frontal	Lt
86	Frontal_Mid_Orb_L	ORBmid.L	Frontal	Lt
87	Frontal_Mid_L	MFG.L	Frontal	Lt
88	Frontal_Sup_Orb_L	ORBsup.L	Frontal	Lt
89	Frontal_Sup_L	SFGdor.L	Frontal	Lt
90	Precentral_L	PreCG.L	Frontal	Lt

국 문 초 록

발달 과정에서의 ADHD 뇌 네트워크의 연구

: 소동물 ^{18}F-FDG PET 및 소아-청소년 fMRI 연구

하승균

서울대학교

융합과학기술대학원

분자의학 및 바이오제약학과

주의력결핍 과다행동장애(ADHD)는 과잉행동/충동 및 부주의로 특징 지어지는 복잡한 뇌발달장애이다. 이러한 ADHD 환자에서는 보상과 동기부여의 측면에서 결함이 있음이 알려져있으며 이에 관여하는 전전두엽-선조체 간의 연결성에서 문제가 있음이 뇌네트워크 분석을 통해서 특징적으로 알려져있다. 이외에 ADHD 뇌 네트워크에서 디폴트 모드 네트워크 (DMN)의 억제가 정상적으로 이루어지지 않는 점 등이 특징적이다. 한편 ADHD 의 원인에 대한 여러 가설이 있는데, 정상적인 성숙이 지연되는 것이라는 가설이 여러 연구 등을 통해서 지지되고 있다. 이에 대한 뇌과학적 증거로는 주로 대뇌피질의 두께 발달에 대한 해부학적 연구 등이 대부분으로 추가적인 기능적 뇌연결성 분석이 필요하다.

이번 연구는 소동물 래트 ^{18}F-FDG PET 영상를 이용한 뇌 대사네트워크(metabolic connectivity)의 종단 연구(longitudinal study)와 사람 fMRI 데이터를 이용한 기능네트워크(functional connectivity) 분석이 수행되었다. SHR 래트가 ADHD 모델로 선택되었으며, WKY 래트가 대조군으로 사용되었고 유년기인 4 주령 및 사춘기의 진입시점인 6 주령에서 ^{18}F-FDG PET 뇌영상을 촬영하였다. 사람 fMRI 데이터로는 공개된 다기관 참여 공공데이터인 ADHD-200 중 가장 규모가 큰 데이터 중 하나인 북경 대학교(Peking University)의 데이터를 12 세를 기준으로 8-12 세의 소아 그룹(정상발달군 85 명; ADHD 42 명,) 및 12-15 세의 청소년 그룹(정상발달군 47 명; ADHD 49 명)으로 나누어 분석하였다.

SHR 래트는 활동성 및 충동성에 대해 다양한 표현형을 보였다. SHR 래트 중 marble burying test, open field test, delay discouting task 등의 행동분석을 통하여서 12 마리의 확연한 충동성 및 활동성을 보이는 SHR 래트를 선별하여 ADHD 래트로 분석하였다. 각 12 마리씩의 ADHD 래트 및 대조군 래트 영상에 대해서 뇌영상을 분석하였으며 복셀기반으로 분석하였을 때 ADHD 래트 및 대조군 래트는 4 주령에서 6 주령으로 발달과정에서 서로 유의한 차이를 보이지 않았다(FWE >0.05). 퍼시스턴트 호몰로지(Persistent homology) 분석법을 이용하여서 뇌대사 네트워크의 발달 과정에서의 변화를 평가하였을 때, 정상 래트 네트워크 분석결과로 4주령에서 6주령으로 발달과정에서 변연계(해마)와 대뇌피질 연결의 강화가 관찰되었다(P <0.05, permutation 10000). ADHD 래트에서는 같은 4 주령의 정상대조군과 비교하여 유의하게 약화되어있던 변연계(내후각피질)-대뇌피질 연결이 6 주령으로 발달함에 따라 강화됨이 관찰되었으며(P <0.05, permutation 10000), 해마와 대뇌피질들간의 연결도

강화되는 경향을 보였다(P <0.10, permutation 10000). 또한, 대조군 4 주령과 ADHD 래트 6 주령의 뇌대사네트워크를 비교하였을 때 양측 시상간 연결이 약화되어있는 것 이외에는 네트워크상의 유의한 차이가 나타나지 않았다. 특징적으로, 4 주령에서 6 주령으로 발달과정에서 ADHD 래트는 '보상 및 동기부여 영역(선조체, 내측전전두엽피질 및 대상피질)'의 모듈화가 정상대조군에 비해서 지연되었다.

퍼시스턴트 호몰로지 방법을 이용하여 소아 청소년기의 fMRI 데이터의 네트워크 분석 결과, 정상발달군은 소아기와 청소년기 간에 기능적 뇌네트워크의 연결성이 뇌 전반에 걸쳐서 유의하게 강화되어 있는 것이 관찰되었다(FDR <0.05). 반면, ADHD 군은 대체로 국소적인 차이를 보였으며, 바코드의 곡선아래면적으로 평가한 총체적인 기능적 뇌네트워크 형성 양상에서 유의한 변화를 보이지 않았다(FDR >0.05). 정상발달군과 ADHD 군의 군별 비교에서는 전반적으로 유의한 차이를 보이지 않았다(FDR >0.05).

마지막으로 래트 대사네트워크 및 소아청소년 기능적 네트워크의 정보처리효율성을 볼륨엔트로피를 지표로 활용하여서 분석하였다. ADHD 래트는 같은 주령의 대조군 래트에 비해서 볼륨엔트로피가 낮았다. 4 주령에서 6 주령으로 발달과정에서 ADHD 래트는 대조군에 비하여 상대적으로 제한적이었지만 발달하는 양상을 보였다. 소아청소년 기능적 네트워크를 분석하였을 때, 정상발달군에서는 연령증가에 따라 볼륨엔트로피가 유의하게 증가하는 상관관계를 보였다(r 0.240, P = 0.006). 대조적으로 ADHD 군은 연령에 따른 볼륨엔트로피의 변화가 유의한

차이를 보이지 않았다(P >0.05). 군별 비교에서는 정상발달군과 ADHD 군에서 유의한 차이를 보이지 않았다(P >0.05).

결론적으로, ADHD 래트 모델의 발달과정상의 대사네트워크 분석을 통해서 ADHD 병발 원인에 대한 '지연된 성숙 가설'을 부분적으로 뒷받침하는 변연계-대뇌피질 간의 연결성의 강화가 지연 및 '보상 및 동기'에 관여하는 뇌영역에서의 모듈화가 지연됨을 확인하였고, 볼륨엔트로피를 통해 전반적인 정보처리효율성의 발달도 지연됨을 확인하였다. 소아청소년 기능적 네트워크 연구에서는 정상발달군의 전반적 뇌연결성 강화에 비해 ADHD 군의 연령 별 차이는 거의 없었으며, 이에 대해 약물치료 등을 통제하는 종단연구(longitudial study) 등이 보완적으로 필요할 것으로 사료된다.

주요어: 주의력결핍 과다행동장애, 지연된 성숙 가설, 뇌 연결성 분석, 퍼시스턴트 호몰로지, 볼륨엔트로피, ^{18}F-FDG PET, fMRI

학번: 2014-30805